

Balancing Repairability and Technical Requirements: A Reliability-Based Optimization Approach for PV Module Design

A.G. Timmers Verhoeven

May 2025, Delft, Netherlands

Abstract

As the solar industry continues to grow, the accumulation of photovoltaic (PV) module waste highlights the pressing need for more circular and repairable designs. Conventional laminated modules are difficult to disassemble and recycle, which limits both material recovery and component reuse. While avoiding the lamination improves disassembly, it also compromises the module's mechanical integrity. This trade-off demands a careful redesign to maintain structural requirements without sacrificing key criteria such as repairability, weight, and cost. This study presents a reliability based optimization approach to redesign the PV module while balancing repairability, weight, and cost constraints. A semi-quantitative relative repairability assessment method, tailored specifically for PV modules, was developed to quantify repairability impacts of design changes. Using Robustimzer software, reliability-base optimization was incoporated to account for uncertain scenarios during the life cycle of the product. Finite Element Analysis and prototype verification ensured compliance with IEC61215 mechanical load standards, achieving an optimized design for mass, repairability and costs simultaneously. As a case study, this methodology was applied to a laminate-free module developed by Biosphere Solar, demonstrating how repairability-focused design can be effectively balanced with structural and economic requirements. The proposed approach offers a scalable framework for advancing sustainable design practices in the PV industry.

Keywords: PV module, FEA, optimization, repairability, uncertainty, reliability, design for sustainability

1. Introduction

The solar industry plays a crucial role in the transition toward a circular economy, offering renewable energy solutions that reduce dependence on fossil fuels and lower carbon emissions. Despite their environmental benefits, Photovoltaic (PV) modules themselves lack circularity. Traditional PV modules consist of several key layers and components working together to ensure efficiency and durability. Figure 1 (*Left*) depicts the design of a traditional laminated PV module. As shown in the figure, the solar cells are encapsulated between two layers of Ethylene Vinyl Acetate (EVA), which enhance the durability and performance of solar modules. These layers hold the cells securely between the glass and the backsheet, while also absorbing shocks and vibrations and shielding the fragile cells and their circuits from damage [1].

While the use of the EVA layer in PV modules initially appears to offer substantial advantages, a major drawback of the laminated design is that it is incredibly challenging to recycle or repair, often requiring energy-intensive processes that are neither cost-effective nor effective at material recovery. This results in a significant waste problem as damaged or end-of-life panels are often discarded rather than refurbished or repurposed. This issue is particularly concerning given that the solar industry is rapidly expanding both in Europe and globally [2]. By 2050, the European Union is expected to generate between 21 and 35 million tonnes of solar panel waste, while globally, the accumulation

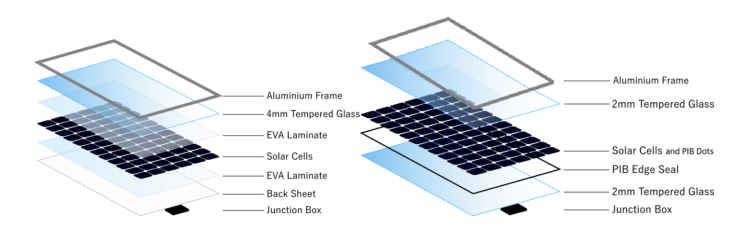


Figure 1. Traditional (Laminated) PV module stack (*left*) and disassemble glass-glass laminate-free Biosphere PV module V1.3 (*right*).



Figure 2. Depictions of adhesive dots placed inside Biosphere PV module.

could reach up to 160 million metric tons [3, 4]. This waste includes valuable materials such as aluminum, copper, glass, and silicon [5].

Several attempts have been made to recover these materials after disposal. For instance, Wambach et al. (2009) demonstrated the technical feasibility of recovering and purifying silicon from end-of-life c-Si PV panels. Their method involved pyrolysis to remove metallization and dopant layers, followed by selective etching to produce a new silicon ingot [6]. A similar process was developed by the Japanese NEDO program through FAIS, which also relies on pyrolysis of the polymers in a conveyor kiln [5]. However, separating materials from the EVA remains a very energy intensive and costly process, often resulting in heavily contaminated recovered materials [7]. Addressing these design limitations of EVA is thus essential for enhancing the sustainability and circularity of solar technologies, ensuring that the industry not only produces clean energy but also minimizes its own environmental footprint throughout the product's lifecycle.

There are several strategies to increase the circularity of a product, which can be summarized in the 9 R's displayed in Figure 3: Refuse, Rethink, Reduce, Reuse, Repair, Refurbish, Remanufacture, Repurpose, and Recycle [8]. Integrating these strategies enables a transition from a linear to a circular economy, maximizing product lifecycles and minimizing waste, with Refuse (R0) being the most favorable and Recover (R9) the least. Since the solar industry provides a far better solution compared to other energy alternatives, it should not be refused or reduced. Instead, the focus should shift toward enhancing reuse and repair rather than solely relying on recycling or material recovery. A few PV module designs focused on improved repairability or reusability can be found in literature, like the NICE technology [9] or the modular PV module proposed by Majdi et al. (2021) [10]. From both repairing and recycling perspective, these designs enables the recovery of entire piece components such a glass, copper tabs, and solar cells at low-cost and with a negligible amount of contamination by other materials, resulting in clean residue-free surfaces [11].

A similar route is adopted by Biosphere Solar. Biosphere Solar is a startup focused on transforming the solar energy industry by developing a repairable and recyclable PV module. They are creating a modular, circular, and transparent PV module using an open-source methodology and sustainable production techniques to promote clean energy accessibility. To enhance the circularity of PV

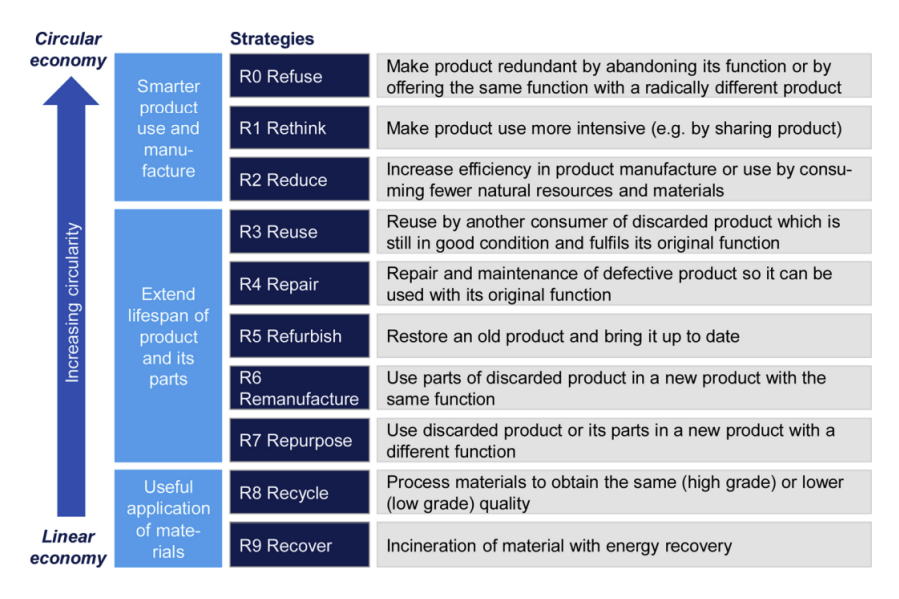


Figure 3. The 9 R's for a circular economy [8].

technology, Biosphere Solar has introduced a panel architecture that eliminates the use of EVA. To avoid lamination, Biosphere Solar's PV modules use a polyisobutylene (PIB) seal around the edge to connect the two glass plates and protect the solar cells from moisture and dust. A schematic comparison between a conventional laminate PV module and Biosphere Solar's Laminate Free module is shown in Figure 1. In order to provide extra strength to the module, the new version (v1.3) is designed with small PIB dots placed between the solar cells to keep them in place and connect them to the glass plates, see Figure 2. In this paper, version v1.3 is used as the reference.

To access and repair or recycle internal components such as the solar cells, the frame is first removed. Next, the edge seal and adhesive dots are cut using a hot knife and wire cutter, allowing the glass layers to be separated and the internal components to be reached. Without the lamination process, this design allows for the reuse, repair and recycling of major components while minimal energy is required for disassembly, as the process involves mechanical separation rather than for instance high-temperature methods. One major drawback of the current design is the limited mechanical strength of the module. According to the IEC61215 standard for PV modules, the module must be able to withstand a minimum static load, a minimum dynamic load and a minimum impact force, representing external forces such as those experienced during transport, storms, or snowfall [12]. However, Biosphere's current module design fails to meet this requirement (see Figure 4). As such, a primary design challenge for Biosphere is to improve the structural integrity of the module to better resist these external loads. At the same time, these improvements should not come at the expense of key factors like weight, cost, and repairability. Iterative trial-and-error approaches to achieve this balance are often time-consuming and costly; for instance, early design iterations aimed at improving repairability led to a significant reduction in mechanical strength and high costs. This highlights the need for a systematic, combined optimization approach that simultaneously considers structural performance, repairability, cost, and mass to arrive at a viable, balanced design.

This challenge is complicated by the absence of a standardized method to evaluate or compare the repairability of solar panel designs. Yet, to effectively design or redesign for repairability, it is crucial to establish a clear and consistent framework for how repairability is assessed.

Another complication is the fact that both modeling and real-world parameters involve inherent

uncertainty. A common engineering response is to apply conservative safety margins to account for these unknowns. However, while this approach increases robustness, it can also result in unnecessary overdesign, adding weight or cost that may not be needed. This is particularly problematic for a startup like Biosphere, where material efficiency and performance are critical. Therefore, this study employs an optimization algorithm that incorporates uncertainty quantification directly into the design process. This allows for a more targeted and efficient balancing of structural performance, cost, weight, and repairability, reducing the need for excessive safety factors and the need for costly trial-and-error approaches while still ensuring reliability. This study addresses two primary research gaps:

- The development of a methodology to evaluate and quantify the repairability of solar modules and to integrate this metric into an optimization framework.
- The implementation of a reliability based optimization algorithm to systematically account
 for uncertainties in the design process of PV modules, thereby reducing the reliance on
 conservative safety margins and minimizing the need for costly trial-and-error approaches.

Biosphere's solar PV module design is used as a case study to demonstrate the applicability and effectiveness of the used methods. More broadly, the proposed approach offers a scalable framework for all solar technology developers, and particularly startups, in making informed design decisions during early-stage product development.



Figure 4. Biosphere PV module design after applying uniform static pressure of 2400Pa.

As a follow-up to this introduction (Section 1), Section 2 introduces general repairability assessment methods and proposes a tailored assessment method for evaluating the repairability of PV module designs. Section 3 provides a short introduction into several reliability based optimization techniques. The used optimization methodology, including the objective function, constraints, and the incorporation of uncertainty quantification through robust optimization techniques is outlined in Section 4. Section 5 describes the method used in this optimization study and Section 6 describes the verification of the finite element model through experimental testing. In Section 7 the optimization results and their interpretation are discussed. In Section 8 the limitations of the study and recommendations for future improvements are addressed. Finally, Section 9 summarizes the key findings of this study in a conclusion.

2. Assessing repairability

2.1 Repairability assessment methods

To effectively improve a product's repairability during (re)design, it is essential to have a clear and precise definition of how 'repairability' will be assessed. During the last few years, in line with the European Regulatory Framework, several initiatives have been introduced with the aim of assessing the level of repairability of different products [13]. The methods described in the literature can be divided into three categories:

- · Qualitative methods that establish pass-fail criteria
- Semi-quantitative methods that allow to compare products within a specific family
- Quantitative methods that use measurable data to evaluate aspects such as the ease of disassembly.

One qualitative method is for example the method developed in 2018 by Cordella et al. [14]. In this research a product-specific checklist of parameters and conditions was developed that positively influence the repairability and upgradability of Energy related Products (ErP) [14]. Within semi-quantitative approaches, the Assessment Matrix for ease of Repair (AsMeR) [15] and the Repair Scoring System (RSS) [16] are the most commonly used [17]. These methods calculate a 'repairability score' by examining the features of a specific product family. This process helps to identify the most appropriate evaluation criteria for that product range, such as key parameters and target components, as well as determine the importance of each criterion. Other frequently used methods are the iFixit methodology, or labels like ONR 192102 [18], EN 45554 [19] and the 'French Indice de Réparabilité' (FRI) [20, 21]. These semi-quantitative methods are usually combined with quantitative methods, such as the 'ease of Disassembly Method' (eDiM) [22], which uses the 'Maynard Operation Sequence Technique' (MOST) to estimate the disassembly time for a component, taking into account the operator's skills and other relevant factors [23].

Given that these methods often need tailoring to specific products, significant research has been conducted to adapt them to particular product categories. For instance, iFixit has devised a method specifically for evaluating the repairability of smartphones [24], while the French Repairability Index (FRI) has applied similar approaches to vacuum cleaners, washing machines, dishwashers, TVs, laptops, smartphones, and lawnmowers [21]. However, no assessment method yet exists that is tailored specifically for the repairability of PV modules. This represents a significant research gap that must be addressed to enhance the circularity of PV module technology. Consequently, a Comprehensive Assessment Framework for Enhancing PV module Repairability has been designed in the next section, providing a tailored method able to compare the repairability level of different PV module designs or different modifications within one design.

2.2 Relative Repairability Assessment Method for PV Module Designs

As most 'repairable' PV modules are still in the concept phase, many quantitative methods prove too detailed for the concept stage, as specifics like the number of screws or disassembly steps are not yet determined. Additionally, quantitative methods often overlook many factors that contribute to 'repairability', as they only account for those that can be measured or calculated [25]. On the other hand, qualitative methods based on pass-fail criteria (e.g. Cordella et al. [14]) only allow to differentiate between 'good' and 'bad' products but not to assess the relative repairability of specific models. Therefore, for the assessment of PV module concepts, the qualitative method proposed by Cordella et al. is adapted to a semi-quantitative method to allow better differentiation between design options while preventing the need of detailed product information as needed in most quantitative methods. This method thus assesses the relative impact of different design changes, rather than relying on a single overall score. It focuses on evaluating how different design options or modifications within a design would affect repairability in relative terms. This is especially useful for *optimizing a design on*

repairability, as it allows designers to make informed trade-offs and prioritize which modifications are most effective for improving repairability.

In Table 1, a list of criteria that influence the repairability of PV modules is presented. This list is based on the generic and non-exhaustive list of criteria for assessing the repairability and upgradability of products developed by Cordella et al. (2019) [26] and is adapted to specifically address PV modules. A key modification includes integrating 'automation' into the Accessibility, Visibility, and Tools criteria, recognizing that PV modules are typically assembled and disassembled by machines. The criterion 'data deletion' has been excluded as it is irrelevant to PV modules. The definition of Technical Skills has been revised to reflect a more realistic scenario where the optimal situation is that the repair can be performed by any technician, rather than by the end-user. This adjustment acknowledges that PV modules are complex systems, and it is more realistic to expect professional technicians, rather than users, to handle repairs effectively in the case of PV modules. The final modification involves incorporating time into the definition of Disassembly and Reassembly. This change acknowledges that while a process may be achievable within a limited number of steps, it is equally important that these steps can be completed within a reasonable time frame. By including time, the definition better reflects the practical considerations of repair efficiency.

Table 1. Repairability assessment criteria with definition.

Criterion	Definition		
Identification of the problem	Causes of all key failures can be established easily because of its evidence (e.g. error codes are provided directly by the product or in the user manual)		
Availability of maintenance and repair information	Maintenance and repair information is provided by the manufacturer (printed or online)		
Technical skills	The repair of key failures can be done by any technician.		
Availability of spare parts	Original and compatible spare parts are widely available to replace parts		
Identification of parts	parts are clearly distinguishable, engraved, marked or labeled for quick identifications and/or replacement		
Disassembly and reassembly of parts	All parts can be disassembled (i.e. remove a part from the product) and reassembled (re-connecting part to product) in a limited number of steps and within limited time span		
Accessibility of parts	All parts are readily accessible (i.e. attainable without requiring for example the pri removal of other components) with tools or machines		
Visibility of fasteners	Fasteners used to assemble parts are visible for either human eye or used machine		
Removability of fasteners and disassembly reversibility	All connections are reversible and reusable		
Repair location limitations	Repair of parts can be done on the spot		
Degree of automation	Repairing process can be fully automated		
Types of machinery and tools needed	Basic machines or tools are needed to disassemble parts		
State after repair/upgrade action	The product functions with no or minimal loss in quality (efficiency and power output) and aesthetics		
Updatability	The product is adaptable to market standards, meaning the product allows users the possibility to replace parts for newer versions available on the market		

Table 2 outlines a relative scoring method based on these criteria. Each criteria is weighted (either 1, 2 or 3) according to its relative importance on repairability. A weight of 1 is assigned if the panel can still be repaired when this criterion is met, though it may require slightly more effort or time. For example, the 'Availability of maintenance and repair information' is assigned a weight of 1, as the lack of this information may make it more challenging for a technician to figure out how to repair the panel, though the repair can still be done. A weight of 2 is given when the absence of this criterion significantly complicates the repair, requiring considerable workarounds. A weight of 3 indicates that repair is practically impossible if this criterion is not met. For example, a weight of

3 is given to 'Disassembly and reassembly of parts' and 'Removability of fasteners and disassembly reversibility' as it is often impossible to repair parts when they cannot be disassembled, removed or reassembled. The weighting factor can be adapted to the application or the aim of the specific design and is therefore a slightly subjective decision for the engineer. However, the weighting is valuable since some criteria are interrelated. For instance, redesigning a concept to simplify the automation of the repair process (which is beneficial) might require more advanced tools (which is less favorable). The weighting factor can therefore help determine whether the overall impact on repairability is positive or negative. The scoring ranges from negative (-1) if the design change has a negative effect of this specific criterion, neutral (0) if no effect, to positive (1) if it positively effects this criterion.

Most methods found in literature typically focus on priority parts rather than all components. These priority parts are generally identified based on criteria such as failure rates, technical or market considerations, or environmental and economic impacts. While this can be useful in later stages of development, the approach proposed in this work does not distinguish between priority and non-priority parts. This is because the method is primarily intended for use in the early design phase, where it is often still unclear which components will ultimately be considered priority parts. At this stage, the dimensions and characteristics of components can vary significantly. For instance, the glass layer could still be doubled in thickness. Thin glass is prone to breakage and would likely be classified as a priority part due to its high failure rate, whereas thicker glass may be significantly more robust and thus not prioritized. Also the environmental impact of a part is hard to estimate in this stage, as this depends heavily on the amount of material used. These quantities are still flexible during early design, which makes it difficult to make accurate assessments about which parts will have the most significant environmental or economic impact. For that reason, the current method takes all parts into consideration equally, making it more suitable for early-stage assessments and optimization purposes where design parameters have not yet been fixed.

Rela	Relative Repairability Assessment Method for PV modules						
Parameter [Weight]	-1	0	1				
Identification of the problem [2]	design parameter limits the ability to establish	An increase in the design parameter has no impact on the identification of the possible causes of key failures	parameter ensures that more causes of key fail-				
		sign parameter has no impact on the availabil- ity of maintenance and	parameter increases the				
Technical skills [1]	parameter increases the reliance on specialized	An increase in the design parameter has no impact on the technical skills needed for repair of parts	parameter reduces the need for specialized				
Availability of spare parts [2]	0 .	sign parameter has no impact on the availabil-					
			Continued on next page				

Relative Repairability Assessment Method for PV modules (continued)						
Parameter [Weight]	-1	0	1			
Identification of parts [1]	An increase in the design parameter causes the parts to be less distinguishable from other parts	An increase in the design parameter has no impact on the identification of parts	An increase in the design parameter causes the parts to be more distinguishable from other parts			
Disassembly and reassembly of parts [3]	,	An increase in the design parameter has no impact on the time and amount of steps needed for disassembly and reassembly of parts	An increase in the design parameter decreases the number of steps or time required for the disassembly and reassembly of parts			
Accessibility of parts [2]	An increase in the design parameter reduces the accessibility of parts for tools or machines	An increase in the design parameter has no impact on the accessibility of parts with tools or machines	An increase in the design parameter increases the accessibility of parts for tools or machines			
Visibility of fasteners [2]	An increase in the design parameter reduces the visibility of fasteners used to assemble parts	An increase in the design parameter has no impact on the visibility of fasteners used to assemble parts	The design increases the visibility of fasteners used to assemble parts			
Removability of fasteners and disassembly reversibility [3]	An increase in the design parameter reduces the reversibility and/or reusability of the connections	An increase in the design parameter has no impact on the reversibility and/or reusability of the connections	An increase in the design parameter increases the reversibility and/or reusability of the connections			
Repair location limitations [1]	An increase in the design parameter limits on-site repairs of parts	An increase in the design parameter has no impact on the possible repair locations	An increase in the design parameter facilitates on- site repairs of parts			
Degree of automation [2]	An increase in the design parameter reduces the automatization possibilities of the repairing process	An increase in the design parameter has no impact on the automatization possibilities of the repairing process	An increase in the design parameter increases the automatization possibil- ities of the repairing pro- cess			
Types of machinery or tools needed [2]	parameter increases the need for more advanced or specialized tools or machines (like tailored machines or product-specific tools) to repair parts	An increase in the design parameter has no im- pact on the types of ma- chinery or tools needed	An increase in the design parameter decreases the need for advanced or specialized tools or machines, meaning more basic tools (like flathead and hex drivers) can be used to repair parts			
pair/upgrade action [2]	An increase in the design parameter has a nega- tive impact on the qual- ity (efficiency or power output) and aesthetics of the product	An increase in the design parameter has no impact on the quality (efficiency or power output) and aesthetics of the product	An increase in the design parameter has a positive impact on the quality (ef- ficiency or power out- put) and aesthetics of the product			
Updatability [2]	An increase in the design parameter limits the pos- sibility to replace parts for newer versions	An increase in the design parameter has no impact on the possibility to replace parts for newer versions	An increase in the design parameter facilitates up- grading parts for newer versions			

Table 2. Method to assess relative repairability between different designs or design variables.

2.3 Repairability of Biosphere's Design Modifications

Biosphere's current PV module design does not provide sufficient mechanical strength and requires significant reinforcement to endure common loads from transport, storms, or snowfall. At the same time, it is essential to minimize any compromise to repairability, as it is the core mission of the company to develop a circular, easily maintainable PV module. Without altering the overall layout, several modifications can be considered to enhance the structural strength of Biosphere's PV module design. Increasing the glass thickness, for instance, can help reduce the risk of breakage. The panel's overall stiffness and strength can also be improved by either adjusting the thickness of the frame or the number of adhesive within the module. Since the highest stress concentrations in the glass and solar cells are expected to occur around the mounting clamps, additional improvements may include enlarging the contact area between the clamps and the frame, or adjusting the panel's mounting position to better distribute loads.

The Relative Repairability Method, described in Section 2.2, is applied to each of these potential design modifications to assess their impact on the overall repairability of the design. In Appendix 1.1- 1.5 the Relative Repairability Assessment Method is applied on several possible design modifications: thicker glass (Hglass1, Hglass2), thicker frame (Hframe), more adhesive dots (Ndots), larger distance between the mounting clamps (Dmounting), and bigger mounting clamps (Wclamp). The Appendices also include the final relative repairability score (RS) of this modification. Figure 5 provides an overview of how these the design variables (Hglass1, Hglass2, Hframe, DdotsX, DdotsY, Dmounting and Wclamp) are defined. The distances DdotsX and DdotsY determine the amount of adhesive dots (Ndots).

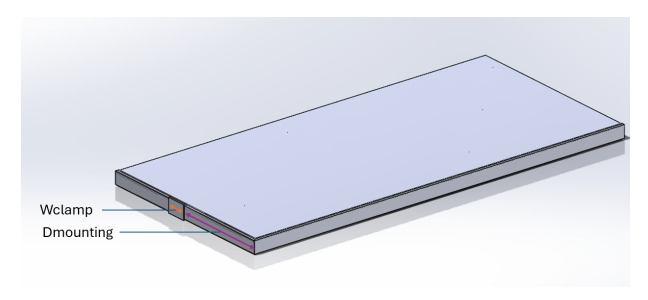
As justified in the Appendices, a thicker glass sheet will likely result in a more repairable design (RS 5/26). This is mainly due to the fact that a thicker glass will less easily break making it easier to carry or transport. A thicker frame, at least within reasonable thicknesses, seems to have limited impact on the overall repairability (RS 0/26). Also the size and the location of the mounting clamps seem to have no noticeable impact (both RS 0/26). Increasing the amount of adhesive dots will result in a significantly lower repairability of the design (RS -8/26). The adhesive dots are not only non-reusable, as for now they also require manual assembly and removal, since no machine has yet been developed that can effectively remove the dot residuals. This significantly increases the disassembly and reassembly time during repair.

This indicated that from a repairability point of view alone, the most effective approach would be to increase the glass thickness and, if necessary, adjust the frame thickness and mounting clamp design to ensure the panel can withstand a minimum load of 2400Pa. However, for a startup like Biosphere, maximizing repairability must be balanced with other key factors such as total cost and weight, which are crucial in determining whether the panel can compete in the saturated solar panel market. Because the trade-offs between these factors are complex and not easily optimized through manual iteration, optimization techniques are applied to systematically identify the best design configuration.

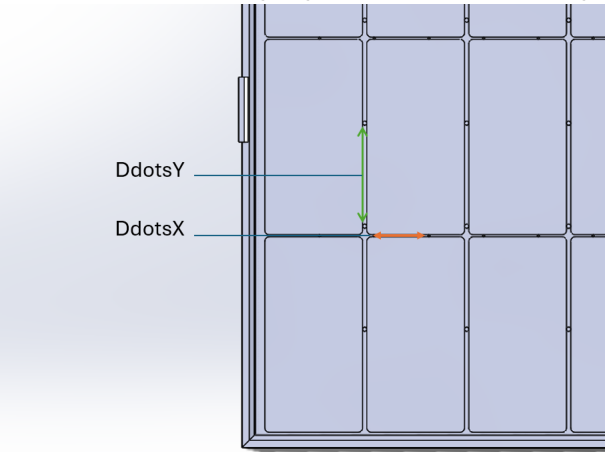
3. Reliability Based Optimization Techniques

Given that this study focuses on a concept-phase design, significant uncertainty exists due to the lack of precise data and extensive experimental validation. In early-stage development it is therefore useful to adopt an optimization approach that can systematically account for these uncertainties.

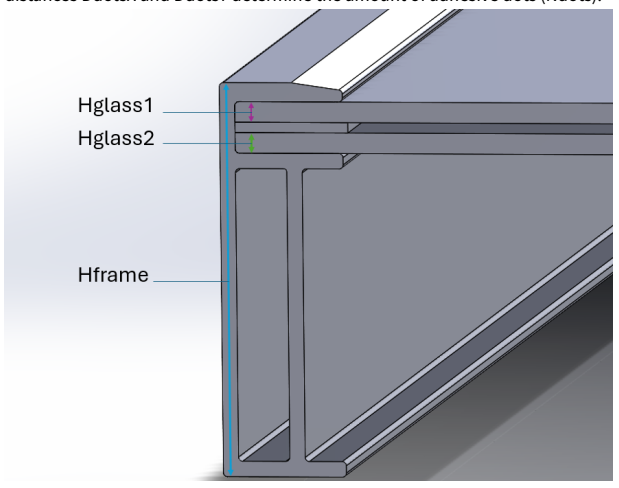
In engineering design, Reliability-Based Design Optimization (RBDO) is used to optimize system performance while accounting for uncertainty in for example loads, material properties, or manufacturing tolerances [27]. These approaches are typically categorized based on how they integrate reliability analysis into the optimization loop. Double-loop methods, such as the Reliability Index Approach (RIA) and Performance Measure Approach (PMA), perform nested loops of optimization



(a) Biosphere PV module showing design variables Wclamp and Dmounting.



(b) Top view of the PV module showing design variables DdotsX and DdotsY. The distances DdotsX and DdotsY determine the amount of adhesive dots (Ndots).



(c) Cross-section of the solar panel, showing design variables Hglass1 (top glass), Hglass2 (bottom glass) and Hframe.

Figure 5. Overview of the design variables.

and reliability evaluation, but are often computationally expensive [28]. To improve efficiency, single-loop methods like Sequential Optimization and Reliability Assessment (SORA) and Decoupled RBDO have been developed, which separate or simplify the reliability calculations during optimization [29]. Furthermore, surrogate-assisted methods reduce computational cost by using response surface models, such as Kriging or polynomial regression, to approximate expensive simulations [28]. While these approaches offer significant potential, their application remains largely confined to specialized research domains [30]. This limited adoption is partly due to the complexity and inaccessibility of existing tools. Their implementation can be complex and often requires custom programming or extensive tuning. Moreover, constructing surrogate models and the use of approximation methods such as Monte Carlo simulations for uncertainty quantification often impose substantial computational time.

To address the limitations in existing optimization workflows, Nejadseyfi developed Robustimizer, a graphical user interface designed for efficient uncertainty quantification, robust optimization, and reliability-based optimization (RBDO) [30]. By combining surrogate modeling with analytic formulations, the software enables fast and accurate exploration of uncertain design spaces without the need for extensive custom coding. At the same time, it facilitates intuitive constraint handling through its graphical user interface. This program is particularly well suited for this case study, due to its demonstrated value in optimization processes aimed at reducing environmental impact particularly in contexts where effectively managing uncertainties is crucial [30].

4. Optimization Framework

The optimization problem in question involves minimizing an objective function while satisfying constraint boundaries and accounting for uncertainties inherent to the design. An overview of the applied optimization framework is presented in Table 3. The next sections provide a detailed breakdown of the optimization framework used to optimize the Biosphere Solar PV Module.

Туре	Expression	Description
Design Variables	x = [Hframe, Welamp, Dmounting, Hglass1, Hglass2, DdotsX, DdotsY]	Design parameters of the PV module and its mounting.
Objective Function	$\min_{\mathbf{x}} F_{obj}(\mathbf{x}) = rcM_{tot}(\mathbf{x}) + rcR_{tot}^{-1}(\mathbf{x}) + rcC_{tot}(\mathbf{x})$	Minimize the total weighted cost, combining mass, inverse reliability, and cost.
Constraint 1	$\mu_{sp1_{glass}}(x) + 3\sigma_{sp1_{glass}}(x) < \sigma_{glass}^{tensile}$	Limit the probabilistic tensile stress in the glass to stay below its strength.
Constraint 2	$\mu_{sp1_{cells}}(x) + 3\sigma_{sp1_{cells}}(x) < \sigma_{silicon}^{tensile}$	Ensure stress in solar cells remains within material limits.
Constraint 3	$\mu_{\delta_{\text{glass}}}(\mathbf{x}) + 3\sigma_{\delta_{\text{glass}}}(\mathbf{x}) < 80 \text{ mm}$	Limit the maximum deflection under load to prevent structural failure.

Table 3. Optimization problem overview with mathematical expressions

4.1 Parameters

Table 4 provides an overview of the design parameters included in the optimization, along with the boundaries maintained for each parameter during the process. These parameters represent all the adjustable elements within the existing Biosphere design that influence stress and deformation in the solar glass (proven to be the most critical component) without requiring an entirely new design concept. While other strategies could further enhance the panel's performance, such as using strengthened (tempered) glass, this parameter is excluded from the optimization process. The reason is that tempered glass improves both mechanical strength and repairability, while having negligible impact on costs and weight. As there is no meaningful trade-off, the use of tempered glass is assumed as a baseline design choice. Additionally, optimizing the panel size could further enhance the panel's performance. In general, smaller panel sizes lead to improvements in strength, repairability, and weight. However, there is a trade-off in terms of cost: deploying many small panels can increase system-level costs compared to using fewer large panels, particularly in solar farm applications. Since Biosphere aims to offer panels in various sizes to meet different application needs and power output requirements, panel size is treated as a discretized variable rather than a continuous optimization parameter.

Parameter	Original value	Lower Bound	Upper bound	Considerations
Hframe	30 mm	10 mm	100 mm	Lower limits set to avoid large computation time. Upper limit set to fit the mounting clamps.
Wclamp	50 mm	35 mm	100 mm	Theoretical limits to fit on mounting rails.
Dmounting	100 mm	0 mm	464 mm	Theoretical minimum and maximum to fit on the frame.
Hglass1	2 mm	2.8 mm	4 mm	Thinner glass is not available for tempered glass [31]. Upper limit is set to 4mm for efficiency considerations.
Hglass2	2 mm	2.8 mm	6 mm	Thinner is not available for tempered glass [31]. Upper limit is set to 6mm for efficiency considerations.
DdotsX	140 mm	20 mm	396 mm	Lower limit set to avoid very large computation time. Theoretical upper limit due to constraints in the 3D model.
DdotsY	100 mm	20 mm	188 mm	Lower limit set to avoid very large computation time. Theoretical upper limit due constraints in the 3D model.

Table 4. Design parameter overview with bounds and considerations.

4.2 Objective function

The aim of this optimization is to reinforce Biosphere's PV module design to better withstand external forces without significantly compromising the panel's repairability, weight, or costs. The proposed modifications must carefully balance these competing objectives. As a result, the objective function is defined as a linear combination of mass, costs, and repairability. However, rather than summing the absolute values, the objective function is a sum of their relative (normalized) changes. This means this approach expresses the objective in terms of percentage change; for example, a 100% increase in total mass would result in an increase of one in the objective function. It is desirable to minimize the objective function.

$$\min_{\mathbf{x}} F_{\text{obj}}(\mathbf{x}) = rcM_{\text{tot}}(\mathbf{x}) + rcR_{\text{tot}}^{-1}(\mathbf{x}) + rcC_{\text{tot}}(\mathbf{x})$$
 (1)

Where F_{obj} is the objective function [unitless, ratio], rcM_{tot} is the relative change in mass [-], rcR_{tot}^{-1} is the additive inverse of the relative change of the Repairability [-] and rcC_{tot} is the relative change

in total costs [-]. Since mass, repairability, and costs are considered equally important, they are combined in the objective function without applying additional weighting factors. Note that this objective function is tailored to the specific priorities of this case study. For other applications or design cases, the objective function may need to be adjusted to best reflect the specific goals of the design. Next sections provide a detailed breakdown of the individual terms that make up the objective function.

4.2.1 Masses

The relative change in mass is equal to:

$$rcM_{\text{tot}}(\mathbf{x}) = \frac{M_{tot}(\mathbf{x}) - M_{0,tot}}{M_{0,tot}} = \frac{\Delta M_{tot}(\mathbf{x})}{M_{0,tot}}$$
(2)

Where $M_{0,tot}$ is the mass of the original Biosphere module V1.3, and the mass $M_{tot}(\mathbf{x})$, is a function of the used parameters (x) shown in Table 4. Both $M_{0,tot}$ and $M_{tot}(\mathbf{x})$ are the total mass of respectively the original panel and the parametrized panel, and are a sum of the masses of all parts within the module (e.g. frame, sealant, cells, electronics etc).

4.2.2 Repairabilities

As discussed in Section 2 it is complex to give an exact number to repairability, as repairability is dependent on many factors (like (dis)assembly time, degree of automization, removability of fasteners, etc.), while a lot is (yet) unknown during the design phase. However, it is easier to estimate the change in repairability; whether a parameter will likely have a positive or a negative effect on these factors. The total change in repairability (rcRtot) is estimated with:

$$rcR_{\text{tot}}(\mathbf{x}) = \sum_{i} (RS_i \cdot rcP_i)$$
 (3)

The Repairability Score (RS) for each parameter is calculated with the Relative Repairability Method explained in Section 2. This estimation is based on the assumption that the relative change in repairability is linearly proportional to the relative change in each variable. However, this relationship may not hold in reality, as more exhaustively discussed in Section 8. Nonetheless, it serves as a simplified approximation for the purpose of this analysis. The term rcP_i is the relative change in parameter i. For example, the relative change in repairability due to a relative change in the amount of adhesive dots, is calculated with:

$$rcR_{Ndots} = RS_{Ndots} \cdot \frac{Ndots - N0dots}{N0dots}$$
 (4)

Where $RS_{Ndots} = -\frac{8}{26}$ as justified in Section 2.3. The total change in repairability due to all parameter changes in the parametrized panel is then the sum of all relative changes in repairability due to the change in each parameter separately.

For the total objective function, the inverse of the repairability (rR_{tot}^{-1}) is used, as the objective function is being minimized while aiming for a maximized repairability. The additive inverse is calculated as:

$$rcR_{tot}^{-1}(\mathbf{x}) = \sum_{i} (-1 \cdot RS_i \cdot rcP_i)$$
 (5)

4.2.3 Costs

To capture cost variations due to design changes, the relative cost is expressed as:

$$rcC_{\text{tot}}(\mathbf{x}) = \frac{C_{\text{tot}}(\mathbf{x}) - C_{0,\text{tot}}}{C_{0,\text{tot}}} = \frac{\Delta C_{\text{tot}}(\mathbf{x})}{C_{0,\text{tot}}}$$
(6)

The term $C_{0,\text{tot}}$ are the costs for the original Biosphere module V1.3, which is a given constant. The term $C_{\text{tot}}(\mathbf{x})$ are the costs of the parametrized module and depends on the parameters listed in Table 4. The total costs are the sum of the material costs, shipping costs, and production costs. The original costs are the sum of the original material costs, shipping costs, and production costs of the Biosphere module V1.3.

$$C_{\text{tot}}(\mathbf{x}) = C_{\text{mat}}(\mathbf{x}) + C_{\text{ship}}(\mathbf{x}) + C_{\text{prod}}(\mathbf{x})$$
 and (7)

$$C_{0,\text{tot}} = C_{0,\text{mat}} + C_{0,\text{ship}} + C_{0,\text{prod}}$$
 (8)

Material costs The material costs are calculated as the sum of the material costs of each part i:

$$C_{\text{mat}}(\mathbf{x}) = \sum_{i} C_{\text{mat}_{i}} \tag{9}$$

The calculation method for the material costs of a part depends on the product type; some materials (e.g., the PIB sealant) are priced per kilogram, while others (e.g., glass or aluminum frame) are usually priced based on area (m²) or length (m) respectively, and are more or less equally priced for each thickness. For the adhesive dots for example, which is made of the material PIB, the material costs are calculated by

$$C_{\text{mat}_{dots}} = c_{PIB} \cdot m_{dots} \tag{10}$$

While for the glass, the material costs are estimated by

$$C_{\text{mat}_{glass}} = c_{glass} \cdot A_{glass} \tag{11}$$

Where m_{dots} is the total mass of all PIB dots and c_{PIB} is the material price pf PIB per kg (\in /kg). A_{glass} is the area of the glass (m²) and c_{glass} is in (\in /m²).

Shipping Costs Shipping costs are dependent on the amount of panels that fit on one pallet. This depends on the thickness of the panel, as all panels are stacked on the pallet on their sides. The space between the panels is minimal; they are tightly stacked with almost no gap in between, separated only by a thin piece of cardboard. As this cardboard has negligible thickness compared to the panel thickness and a lot of panels fit on the pallet, the number of panels that fit on a pallet is more or less linearly dependent on the frame height of the panel. Consequently, the shipping costs are also approximately linear with respect to the frame height H_{frame} (in mm). Assuming this relationship is linear, one can write:

$$C_{\text{ship}}(\mathbf{x}) = s \cdot H_{\text{frame}}$$
 (12)

where s is a proportionality constant (in \leq / mm). Note that this estimate applies only to small-scale orders, as for small amounts of PV modules (relevant for Biosphere at this stage) the cost is paid per

pallet, while for larger amounts the shipping costs are typically calculated per container rather than per pallet. When scaling up, this estimate should be reconsidered.

Also note that, in practice, the number of panels per pallet must be rounded down to a whole number; if 4.5 panels would fit, only 4 can actually be shipped. While this introduces a small stepwise (non-linear) behavior in the cost function, its effect is negligible. This is because a typical pallet holds a relatively large number of panels (at least 36 or more), meaning that the rounding error becomes proportionally small and the linear approximation remains valid for the purpose of optimization.

Production Costs The production costs are defined as the sum of manual labor expenses and machinery and equipment costs. The production in Biospheres case, is mainly done manually in this early stage. Costs related to supporting equipment or utilities, such as electricity, are assumed to be independent of the design parameters and are therefore excluded from this optimization. Consequently, the production costs for a single Biosphere PV module are estimated based on the number of workers required, the time each worker spends per module, and their corresponding hourly wages.

4.3 Constraints

The constraints of the optimization problem are based on the IEC61215 standard for PV modules [12]. According to this standard, a PV module must be able to withstand a static uniform pressure of 2400 Pascal on the front glass without causing visual damage to the panel. To meet these requirements, several constraints are imposed on the model. First, the *maximum* first principal stress in the front glass due to the uniform pressure of 2400 Pa, denoted by sp1_{glass}, must remain below the tensile strength of the glass. Due to uncertainties in the applied load (see next Section), the calculated stress in the glass exhibits a statistical distribution rather than a single deterministic value. To ensure a conservative yet realistic safety margin, the stress constraint is formulated using a reliability based constraint. Specifically, the upper bound of the stress distribution is approximated by adding three times the standard deviation to the mean stress value. This corresponds to a 99.7% confidence level under the assumption of a normal distribution. The resulting expression ensures that, with high probability, the stress in the glass remains below its material tensile strength:

$$\mu_{\text{sp1}_{\text{glass}}}(\mathbf{x}) + 3\sigma_{\text{sp1}_{\text{glass}}}(\mathbf{x}) < \sigma_{\text{glass}}^{\text{tensile}} \tag{13}$$

Similarly, the *maximum* first principal stress in the silicon solar cells due to this pressure, sp1_{cells}, must stay below the tensile strength of silicon:

$$\mu_{\text{sp1}_{\text{cells}}}(\mathbf{x}) + 3\sigma_{\text{sp1}_{\text{cells}}}(\mathbf{x}) < \sigma_{\text{silicon}}^{\text{tensile}}$$
 (14)

Finally, the maximum deflection of the glass, δ_{glass} , must not exceed a certain limit. This is to prevent the glass from touching the underlying ground. For the Biosphere PV module design V1.3, this happens at a deflection of 80 mm.

$$\mu_{\delta_{\text{glass}}}(\mathbf{x}) + 3\sigma_{\delta_{\text{glass}}}(\mathbf{x}) < 80 \text{ mm}$$
 (15)

Only the stresses in the glass and solar cells are evaluated, as in earlier tests within Biosphere these are proven to be the most critical components in the design. The material properties used, including tensile strengths, are listed in Appendix 2. Note that for the scope of this paper, only the static forces are taken into account. For later research it is recommended to also include constraints for the stresses and deformations due to dynamic, impact and potentially thermal loads.

4.4 Noises

Several factors contribute to uncertainty in the optimization problem, particularly regarding the uniform pressure applied to the top glass of the PV module. First, real-world conditions and testing setups can introduce slight variations in the way pressure is applied, such as uneven loading or equipment inaccuracies causing the actual load to deviate from the intended value. Second, 3D modeling inherently approximates reality. Geometric simplifications and numerical limitations (e.g., finite mesh size) introduce modeling errors. Third, material and manufacturing inconsistencies such as variations in surface texture, flatness, or internal structure can lead to different stress distributions under identical loading conditions [32].

Therefore, when analyzing or simulating the behavior of a solar module under load, it is both realistic and more robust to account for uncertainties in the applied load. Instead of assuming a fixed pressure, the pressure applied to the model (p) is therefore expressed as:

$$p = 2400[Pa] * Nl \tag{16}$$

Here, N_l represents the noise on the load, which can follow various distributions (e.g., normal, uniform, log-normal). Estimating the shape and magnitude of this noise distribution is challenging, especially in the early design phase where experimental data is scarce. To address this, real-life prototype testing was conducted to gain insight into the variability in output responses. The observed deflection data from these tests was then used to approximate the corresponding input noise by comparing it with simulated outputs using different candidate distributions for N_l . This comparison was performed using COMSOL's *Uncertainty Quantification* module. This study quantifies how uncertainty in input parameters (in this case, N_l) propagates to a specific quantity of interest. Here, the maximum deflection of the glass. It estimates the probability density function (PDF) of the output using a Monte Carlo method supported by a surrogate model, reducing computational cost. A Kernel Density Estimation (KDE) is used to approximate the resulting PDFs.

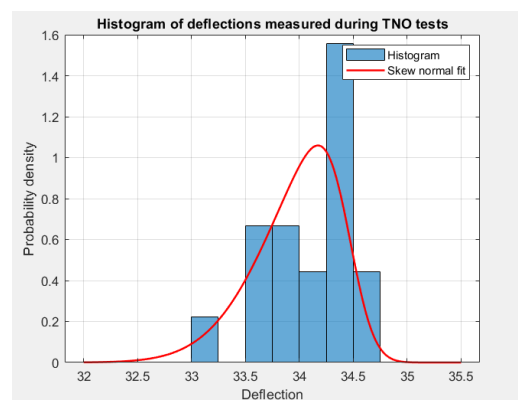
By tuning the input distribution of N_l , a match was found between the simulated output and the real-life measurements. A normal distributed N_l with mean $\mu_{Nl}=1.03$ and standard deviation $\sigma_{Nl}=0.013$ yielded a predicted deflection distribution with a mean $\mu_{def}=34.0$ mm and standard deviation $\sigma_{def}=0.41$ mm which closely matches the experimental results.

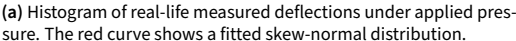
Figure 6a shows the histogram of the measured deflections under pressure, with a red curve representing a skewed normal fit. Figure 6b presents the simulated deflection distribution using the above-defined noise. While this approach improves the realism of the uncertainty modeling, one noticeable difference is that the real-life measurements exhibit slightly more skewness than the simulated data (see also Section 8).

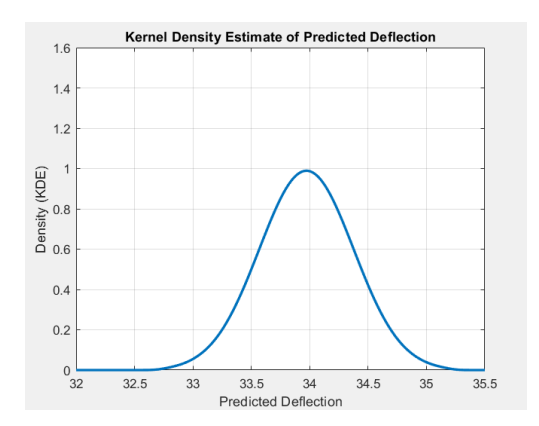
Note that the masses and dimensions used in the optimization are estimated to be reasonably accurate; hence, no noise is applied to these parameters. Although there are known limitations in estimating both the Repairability Score and the exact Costs, these are not incorporated into the noise modeling within the optimization framework, due to the uncertainty associated with their potential fluctuations.

5. Method

In order to do the optimization, a parametrized 3D model of the Biosphere PV module was built in Solidworks. Next, a Livelink was created to connect the Solidworks model to COMSOL Multiphysics which was used to perform the Finite Element Analysis (FEA). The Finite Element Analysis was done for the PV module with the uniform pressure of 2400 Pa on the front glass of the PV module, similar to the real life testing, while the mounting clamps were fixed in place. To decrease the







(b) Kernel Density Estimation (KDE) of simulated deflection using normally distributed load noise ($N_l \sim \mathcal{N}(1.03, 0.013)$).

Figure 6. Comparison of real-life and simulated deflection distributions under load uncertainty. Both distributions show a similar mean deflection ($\mu_{def} = 34.0 \text{ mm}$) and standard deviation ($\sigma_{def} = 0.41 \text{ mm}$). However, the experimental data exhibits noticeable skewness, whereas the simulated KDE assumes a symmetric normal distribution.

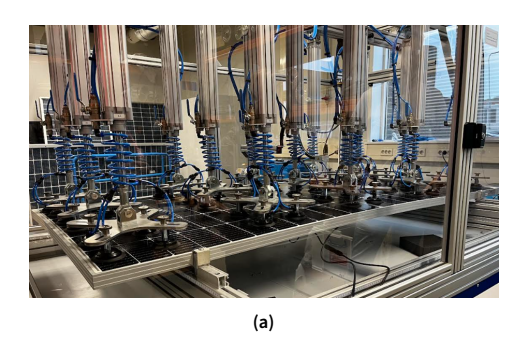
computational time, only a quarter of the panel was modeled and a symmetry was applied along the symmetry planes of the design. Assuming the glue connections will not deadhere during loading, the glue connections were modeled as 'bonded pairs'. The mesh used for the FEA was built using the default Physics-Controlled mesh settings. These settings, depending upon the physics involved in the model, adjust the mesh based upon the geometry, the applied domain and the boundary conditions within the physics as well as the materials properties [33]. The mesh size was progressively reduced until the model's deformation results showed convergence, as detailed in Appendix 14. The 'finer' mesh setting was ultimately selected to balance computational efficiency with adequate simulation accuracy. The 3D model was validated by comparing its predicted deflections with those measured in real-life experiments under equivalent loading conditions.

For the optimization, the optimization program Robustimizer made by O. Nejadseyfi (2025) was used [30]. After the design variables and the noise variables were defined in the user interface, a structured set of parameter combinations was created: the Design Of Experiments (DOE). The DOEs were created via Latin Hypercube Sampling (LHS) and were normalized to improve the numerical stability. These DOEs were then imported into COMSOL to perform the Finite Element Analysis and compute the stresses, deformations and objective function for each DOE. These model evaluations were then imported back in Robustimizer. Using the Gaussian Process, a Surrogate model was fitted to the DOE results to act as an inexpensive approximation of the real system. This allows uncertainty quantification without the need to rerun full models. Leave-One-Out Cross-Validation (LOOCV) was performed on the surrogate model to enhance its predictive accuracy. Due to its efficiency and accuracy, the Sequential Quadratic Programming (SQP) method was selected to identify the optimum design configuration. Using analytical formulations, Robustimizer computed both the mean and standard deviation of the response. To improve surrogate model accuracy, new DOE points were iteratively added near the predicted optimum. This refinement process was continued until the optimum parameter values stabilized.

6. Verification

To validate the results of the finite element analysis (FEA) conducted using the COMSOL model, physical experiments were performed in collaboration with the Dutch research institute TNO. These experiments were designed to closely follow the procedures outlined in the IEC61215 standard for

mechanical load testing of photovoltaic (PV) modules. However, as the application of a full 2400 Pa static load caused immediate failure of the module (see Figure 4), the applied load for verification was reduced to 1000 Pa to prevent damage and allow for meaningful comparison. The mechanical load was applied using a vacuum-based suction setup (see Figure 7a), which exerted pressure on the front glass surface of the PV module. Deflection was measured 10 seconds after load application using a laser displacement sensor positioned at a defined location: 175 mm from the center of the panel (see red dot in Figure 7b). To ensure fidelity in the comparison, the COMSOL model was configured to replicate the loading conditions used in the experiment, including the exact positions of the suction cups. The simulation results were then evaluated at the same probe point as in the experimental setup. The test was repeated 18 times on each of two PV modules with identical designs, in order to assess the variability both within and between the samples.



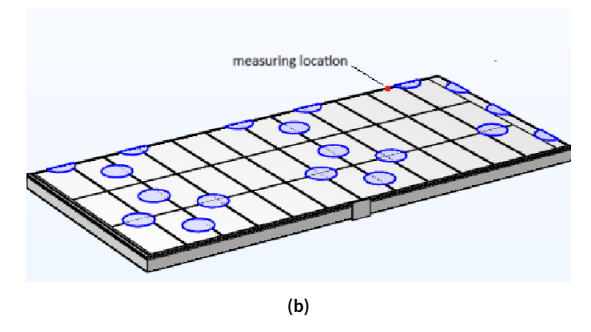


Figure 7. (a) Experimental setup using suction cups to apply 1000 Pa pressure on the PV module. (b) Corresponding COMSOL model showing pressure locations and measurement point. Due to symmetry, only one-quarter of the module is simulated.

The simulated displacement field is shown in Figure 8. The maximum simulated deflection was 33.7 mm at the center, and 33.2 mm at the measurement location used in the experimental setup. Table 5 presents the comparison between simulated and measured deflections, showing a average deviation of 2.4%. These discrepancies are within acceptable margins, especially considering that the variation between the two physical panels, and even between repeated measurements on the same panel, is of similar magnitude.

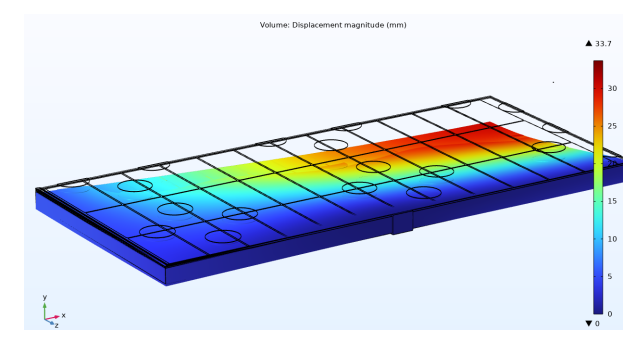


Figure 8. Simulated deflection of the quarter model under 1000 Pa loading.

In addition to deflection, the simulation also assessed tensile stress in the solar cells (see Figure 9a). Several regions, particularly near the long edges, showed stress levels exceeding the tensile strength of crystalline silicon (200 MPa, see Appendix Appendix 2), indicating a risk of microcrack formation. To confirm this prediction, Electroluminescence (EL) imaging was conducted before and after testing. Figure 9b shows the results, where dark spots on the post-test image confirm the presence

Table 5. Comparison of deflection results between experimental (TNO) and simulated (COMSOL) data. The deflection measured at TNO is the average of 36 measurements.

	TNO (Experimental)	COMSOL (Simulated)	Average Deviation [%]
Deflection [mm]	Mean: 34.0 mm Standard deviation: 0.41 mm Range: 33.0–34.5 mm	33.2	2.4%

of microcracks formed during loading. However, it must be noted that the largest observed crack did not align exactly with the location of highest simulated stress, but appeared offset to the right. One possible reason for this discrepancy is the simplifications made in the model (for example, the omission of wires and electronics); see also Section 8.

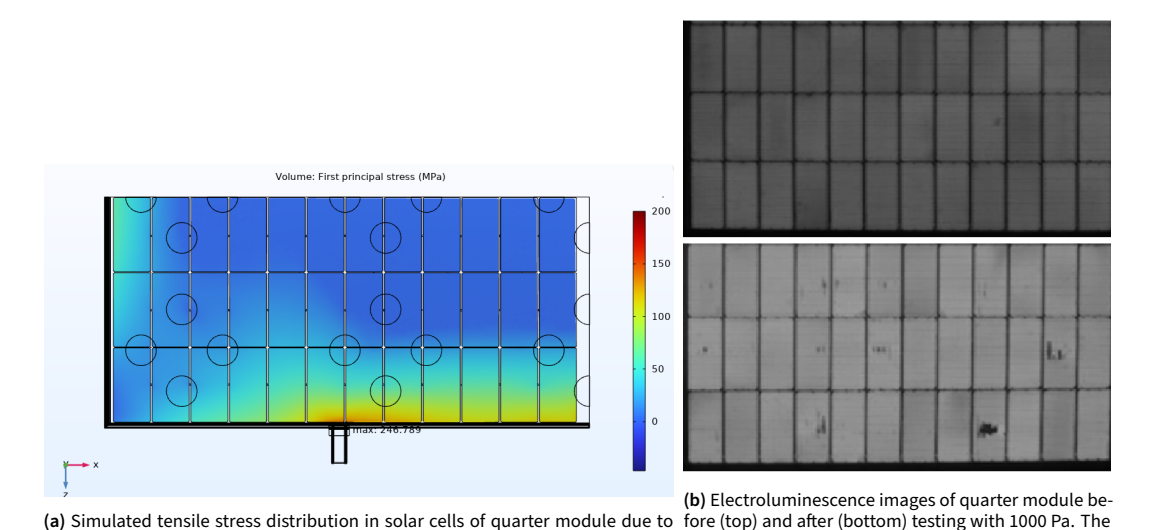


Figure 9. Validation of simulated stress predictions with real-life EL testing.

7. Results

To determine the optimal design configuration of the Biosphere PV module, the optimization framework described in Section 5 was applied. The initial optimization run was performed using 70 DOEs. Subsequently, three additional infill points were incorporated iteratively to refine the solution until the optimum stabilized, see Appendix Appendix 4.

uniform pressure of 1000 Pa. Red zones exceed the maximum tensile stress of 200 same mounting configuration is used as in (a). Dark spots

indicate micro-crack formation.

7.1 Surrogate model and verification

Based on the output from the simulations, a surrogate model was constructed. Using the frame and the (top) glass thickness as an example, Figure 10 presents the surrogate model predicting the tensile stress in the solar cells as a function of parameters Hframe and Hglass2. As expected, increasing either parameter reduces cell stress. However, an important observation is that frame thickness has a considerably stronger effect on stress reduction than glass thickness. This suggests that, for minimizing cell stress, prioritizing an increase in frame thickness is much more effective than increasing the glass thickness.

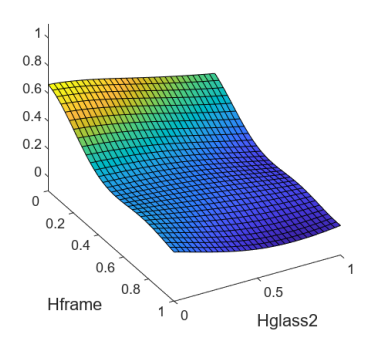


Figure 10. Surrogate model prediction of the tensile stress in the solar cells as a function of frame thickness (*Hframe*) and top glass thickness (*Hglass2*). The plot illustrates that while increasing either parameter lowers cell stress, the frame thickness has a substantially stronger influence on stress reduction than the glass thickness.

Leave-One-Out Cross-Validation (LOOCV) results indicate that the surrogate model for the main response (objective function) has good predictive performance, indicating a reliable surrogate model (see Figure 11a). This was expected due to the linearity in the objective function. Additionally, the surrogate models for the deformation constraint 11b, the stress in the glass (Figure 11c) and the stress in the solar cell (Figure 11d) exhibit sufficient accuracy.

7.2 Simulation results

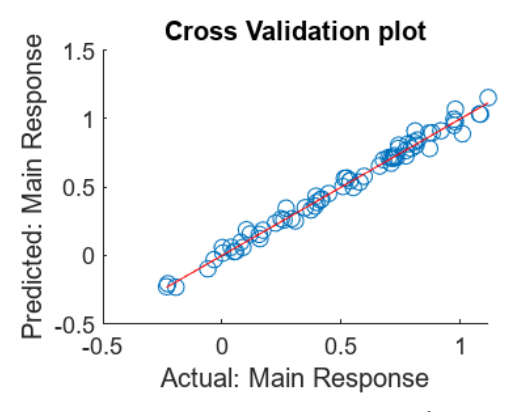
In Figure 12, the effect of the frame thickness (Hframe) and top glass thickness (Hglass2) is again presented as an example. Figure 12a illustrates the influence of the frame thickness on the three objective function components: mass (blue line), repairability (red line), and cost (yellow line). Figure 12b shows the corresponding effect on the constraints, specifically the stresses and deformations.

From Figure 12a, it can be observed that increasing the frame height has a substantial impact on cost, while its effect on mass is minor and its influence on repairability is negligible. This is because a thicker frame slightly increases material usage but considerably raises shipping costs. Conversely, Figure 12b demonstrates that frame thickness significantly affects the stresses in the solar cells and the overall panel deformation. Importantly, the marginal benefit of increasing frame thickness is greatest at lower thicknesses; as the frame becomes thicker, additional increases yield progressively smaller reductions in stress and deformation. From Figure 12c on the other hand, it can be observed that increasing the glass thickness has a positive effect on the repairability of the module but also a high effect on the mass of the entire PV module. It has no effect on the costs of the module, as the price of glass is usually the same for different glass thicknesses. Figure 12d indicates that the glass thickness affects the stresses in the solar cells and glass, and a slightly lower but visible effect on the overall panel deformation. Overall, to increase structural strength, using a thicker frame is more efficient in terms of weight, whereas thicker glass is generally more economical and benefits repairability.

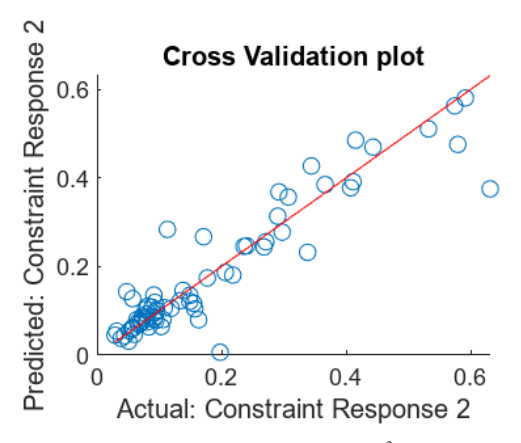
7.3 Optimum design parameters

Table 6 summarizes the found optimized parameter values for the Biosphere PV module design.

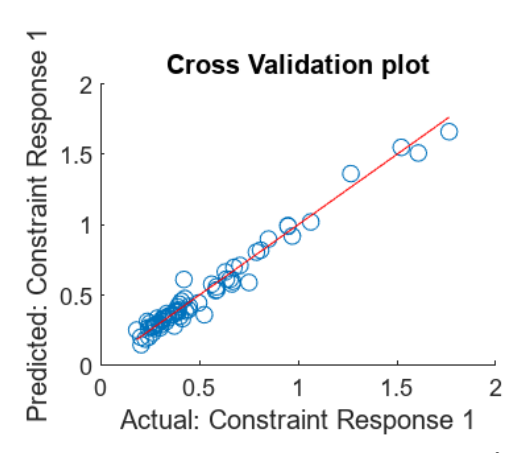
Several notable observations can be made regarding the resulting optimal configuration. Firstly, the optimized frame height is almost similar (only 9.3% decrease, see also Table 6). This outcome was expected, as increasing frame thickness has a significant influence on the structural strength of the module but also significantly increases the shipping costs of the module. Secondly, the optimization resulted in a minimal number of adhesive dots (20 in total, a decrease of 94%), with a strong preference for larger dot sizes. Since both small and large adhesive dots contribute equally to



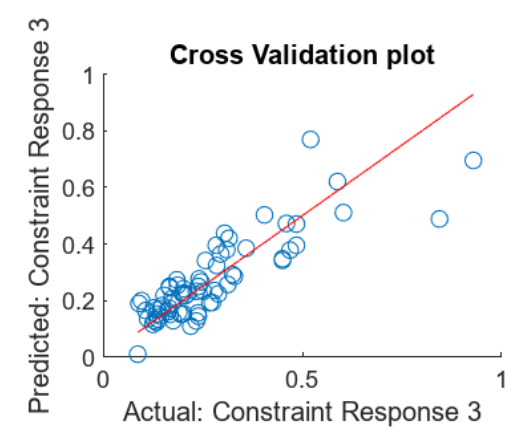
(a) LOOCV for the objective function (RMSE: 0.03885, R^2 : 0.9879). Predictions closely match actual values, indicating a reliable surrogate model.



(c) LOOCV for stress in glass (RMSE: 0.05674, R^2 : 0.8637). The model demonstrates sufficient predictive performance.



(b) LOOCV for the deformation constraint (RMSE: $0.05523,\,R^2$: 0.9716). The model demonstrates good predictive performance.



(d) LOOCV for stress in solar cells (RMSE: 0.08496, R^2 : 0.7188). The model demonstrates sufficient predictive performance.

Figure 11. Leave-One-Out Cross-Validation (LOOCV) performance of the surrogate models used in the optimization framework. Predictive performance is indicated by the Root Mean Square Error (RMSE), which should be close to zero, and the coefficient of determination (\mathbb{R}^2 , quantifying how well the predicted values correlate with the true values), which should be close to one. The objective function and deformation constraint models show high reliability, while the stress models for glass and solar cells show acceptable but slightly lower accuracy.

Table 6. Optimized design parameter values for the Biosphere PV module and their relative change compared to version V1.3.

Parameter	Hframe	Wclamp	Dmounting	Hglass1	Hglass2	DdotsX	DdotsY
Optimum [mm]	27.2	63.9	0.0	3.4	2.8	396.0	177.1
Relative change	-9.3%	+27.8%	-100%	+70%	+40%	+183%	+77%

the repairability score, the optimizer favors larger dots due to their superior mechanical performance in stress mitigation. The glass thickness is also increased compared to the original design, aligning with expectations. Thicker glass not only enhances structural performance and reduces deformation but also improves repairability by reducing fragility. However, the optimizer avoids excessively thick glass, balancing these benefits against the associated weight penalty. The clamp width is increased (27.8%) and moved to the corner of the PV module so optimally reduce the stress around

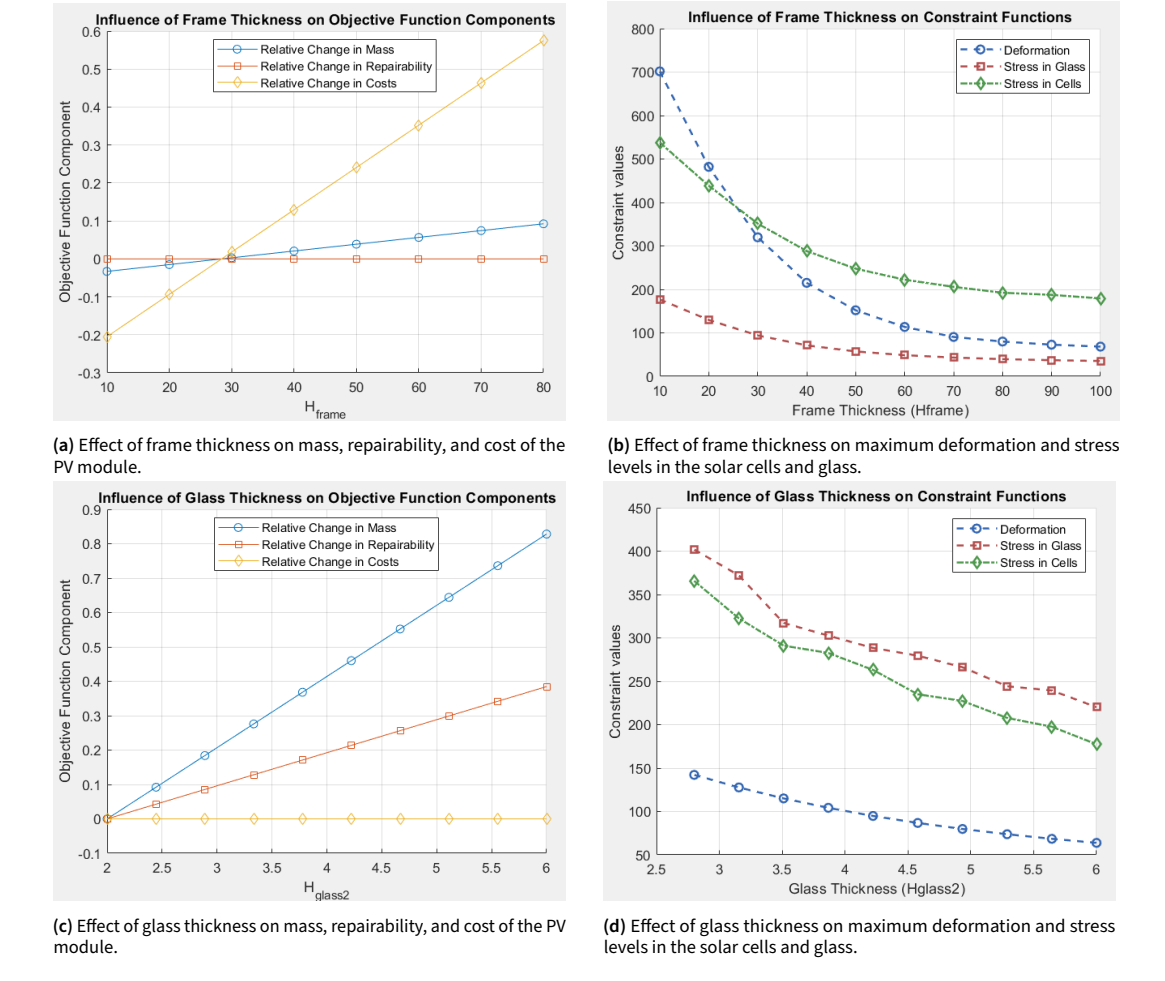


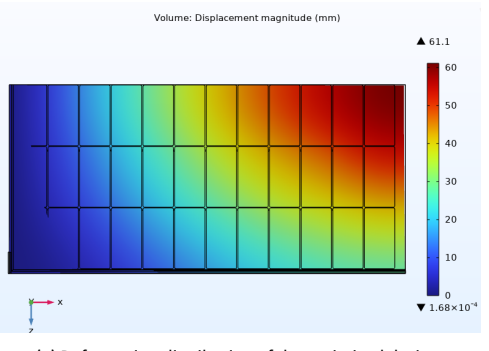
Figure 12. Influence of Frame Thickness (Hframe) and Top Glass Thickness (Hglass2) on Objective Functions and Constraints.

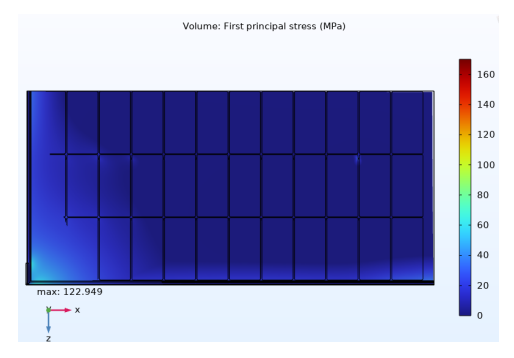
the mounting clamp.

These parameters altogether achieve an objective function value of -0.0928 while satisfying the imposed constraints on deformation and tensile stresses within both the solar cells and glass layers, see also Figure 13.

Although the optimization aims to minimize the objective function (Fobj), the optimal value is close to zero. In theory, a significantly negative Fobj would indicate an overall good improvement in mass, repairability, and cost relative to the reference design. However, such a result is practically unrealistic as the original design fundamentally lacks the mechanical strength to meet the required strength conditions. A design yielding a large negative Fobj would likely be structurally insufficient. Therefore, this slightly negative Fobj reflects the necessary trade-off: the module must be reinforced to endure a static load of 2400 Pa, resulting in moderate increases in weight and cost, with some impact on repairability, compared to the original Biosphere design baseline.

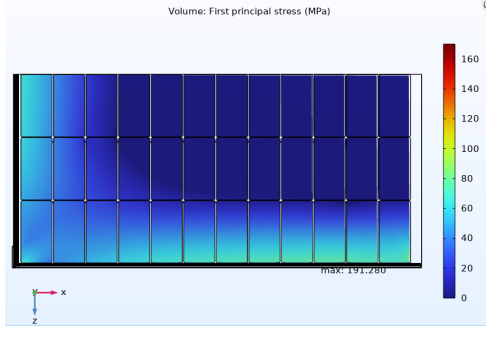
Table 7 presents a comparative overview of the key characteristics of a conventional laminated PV module, the current Biosphere V1.3 design, and the optimized Biosphere V1.3 module. The optimized module demonstrates a substantial improvement in repairability, primarily due to the





(a) Deformation distribution of the optimized design.

(b) Stress distribution in the solar glass for the optimized design.



(c) Stress distribution in the solar cells for the optimized design.

Figure 13. Simulation results of the optimized Biosphere PV module. Note that only a quarter of the module is displayed.

reduction in adhesive dots and the increase in glass thickness. These changes result in fewer irreversible and difficult-to-disassemble connections, as well as more robust and accessible components. Furthermore, the optimized design incurs marginally lower costs than the original V1.3 version, owing to reduced consumption of PIB for adhesive dots and aluminum for the frame, along with slightly lower shipping costs due to a more compact frame configuration. Finally, the optimized module exhibits significantly enhanced mechanical strength compared to the original Biosphere V1.3 design; however, this improvement comes at the cost of increased overall weight, with the module mass rising by approximately 45%.

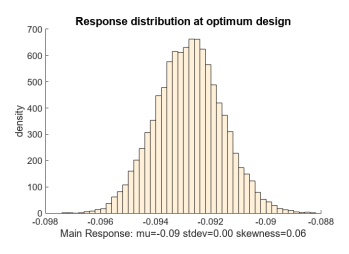
Table 7. Comparison of key characteristics for the traditional laminated PV module, the current Biosphere V1.3 design, and the optimized Biosphere V1.3 module.

Parameter	arameter Traditional PV Module		Traditional PV Module Biosphere V1.3		Optimized Biosphere V1.3
Structural static strength Passes IEC 61215 standard		Fails IEC 61215 standard	Passes IEC 61215 standard		
Repairability	Nearly impossible	Possible in some cases	Achievable in most cases (51% higher than V1.3)		
Mass 37.9 kg/module		32.5 kg/module	47.2 kg/module (45% higher than V1.3)		
Cost	Not available	_	6% lower than V1.3		

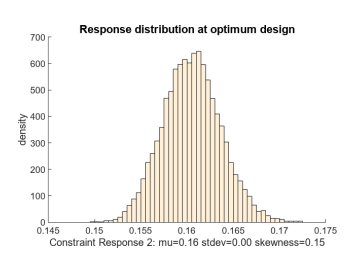
7.4 Uncertainty Quantification at Optimum Design

To assess the reliability of the optimal design under the input uncertainty, a Monte Carlo simulation was performed using the surrogate model. Figure 14 displays the outcome distributions for the three constraint functions evaluated at the optimized design. Each histogram shows how often certain response values are expected to occur in the simulation, with the horizontal axis representing the

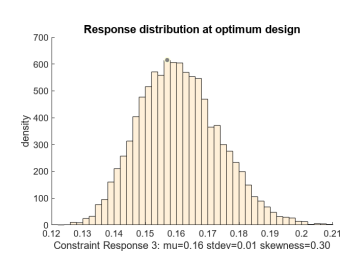
constraint response value and the vertical axis showing the frequency. As can be seen in Figure 14a, Figure 14b and Figure 14c, the Monte Carlo distribution for all three constraints is relatively symmetric and narrow, confirming robust satisfaction of these constraints and demonstrating that the optimized design performs reliably under uncertainty.



(a) Response distribution for the deformation constraint. The distribution is narrowly distributed and symmetric, demonstrating stable constraint satisfaction.



(b) Monte Carlo results for the glass stress constraint. The distribution is narrowly distributed and symmetric, demonstrating stable constraint satisfaction.



(c) Stress response distribution in the solar cells. The values remain narrowly distributed and symmetric, demonstrating stable constraint satisfaction.

Figure 14. Monte Carlo simulations of the objective and constraint functions at the optimum design, quantifying the robustness of the solution under input uncertainty.

8. Limitations and Recommendations

8.1 Repairability Assessment Method

One significant limitation of the applied repairability assessment method is its inherent subjectivity. The weighting factors, which determine the relative importance of each criterion, are slightly subjective and depend on the aim and judgment of the engineer conducting the assessment. This subjectivity can also extend to scoring criteria, such as what constitutes a 'clearly' visible fastener or an 'accessible' component. As a result, different evaluators might arrive at slightly different scores for the same design. Further research is required to refine the weighting factors, particularly to better understand which aspects of repairability are most critical and which may be less relevant. Another methodological limitation lies in the assumption of linearity. The method presumes that the impact of a parameter on repairability is linear: i.e., doubling the parameter results in double the effect. In reality, these relationships are likely to be non-linear, which may lead to different outcomes in the optimization. Further research is recommended to accurately characterize the relationship between specific design parameters and their impact on repairability.

8.2 Modeling and Verification

The 3D model has several simplifications that introduce limitations. Certain components such as wiring, electronics, and cutouts in the glass have been omitted to reduce modeling complexity. Additionally, the frame geometry has been slightly simplified. Although validation has shown that these omissions do not significantly affect static stress results, their influence might be more critical in dynamic or thermal analyses. The verification of the model introduces its own uncertainties. The validation tests at TNO could only measure the deflections at a single location with limited accuracy (>0.25mm). Moreover, there might be some inaccuracies in the applied pressure due to equipment limitations. Only two panels were tested, and large deviations were observed not only between seemingly identical panels, but even between measurements on the same panel. Additionally, during repeated tests on the same panel, a slight increase in measured deflection was observed over time. This may be attributed to prior testing-induced micro-cracks in the solar cells, which could have reduced the overall stiffness of the panel. For future studies it is strongly recommended to do more tests with a larger number of panels and ideally with multiple types of measurement equipment to identify outliers or systematic errors. Allocating additional time and resources to the experimental

testing would substantially enhance the reliability of the verification results. Improved verification accuracy can, in turn, lead to more precise optimization outcomes, potentially reducing the need for costly and time-consuming design iterations later in the development process.

8.3 Optimization Method and Robustimizer Software

The Robustimizer software used in this study also presents limitations. Due to computational time constraints, only a limited number of DOEs could be executed. To address this, the number of DOEs was gradually increased until the expected improvement of the optimization outcomes began to converge, providing a reasonable trade-off between accuracy and computation time. Nonetheless, the surrogate modeling approach inherently introduces approximation errors and can never fully replicate the true performance. Therefore, while the results are indicative, they should be interpreted with awareness of the underlying model simplifications.

8.4 Scope and Time Constraints

The scope of this research was restricted to evaluating static loading conditions. However, for a comprehensive mechanical analysis of PV modules, dynamic and impact loading as well as thermal stresses should be included. These additional effects could significantly alter the design trade-offs and optimization outcomes. For instance, different glass thicknesses for top and bottom glass could result in high thermal stresses within the PV module, potentially shifting the optimal configuration toward equal glass thicknesses to minimize internal stress differentials. Also, incorporating dynamic loads into the optimization framework could shift the optimal design toward configurations with a greater number of adhesive dots. Unlike the static load test, which applies only compressive (pushing) forces, the dynamic load test specified in the IEC61215 standard subjects the module to alternating tensile and compressive forces [12]. This bidirectional loading increases the mechanical demands on the adhesive bonds, potentially necessitating more or stronger adhesive connections to ensure structural integrity.

Furthermore, while this study focused exclusively on repairability as a circularity metric, future research could expand the scope to include other key aspects such as recyclability, reuse, and remanufacturing potential for a more holistic approach.

8.5 Cost Estimation

The costs estimations used for the objective function introduce limitations due to several reasons. First of all, the cost estimation formulas are simplifications. For example, the cost of glass is assumed to scale linearly with surface area and to be independent of thickness, even though in practice the cost per square meter can vary slightly with thickness due to differences in material use and processing. A similar assumption is made for the frame, where a fixed cost per meter is used, overlooking possible variations related to frame height. While these simplifications make the cost model manageable during the early design phase, they do introduce approximation errors. Additionally, some uncertainty occurs due to the fact that costs naturally fluctuate over time, depending on market dynamics such as supply and demand. Also, costs are affected by broader economic or political developments like policies, geopolitical conflicts etc., which can cause sudden price changes [34, 35]. Finally, costs typically decrease when scaling up production, meaning that the current cost estimates may not accurately reflect future large-scale production scenarios. It is advisable to continuously monitor cost fluctuations and develop a design that remains adaptable, enabling timely adjustments in response to changing economic conditions.

8.6 Uncertainty in Noise Estimates

To account for the uncertainties in optimization problem, a noise factor was incorporated into the input: the applied pressure was assumed to have a certain distribution rather than being a deterministic value. However, the precise estimation of the distribution and magnitude of this noise also had its limitations. The input noise was roughly estimated using an uncertainty propagation study, calibrated against real-life experimental results. However, due to the significant limitations of the verification process (see Subsection 8.2), the accuracy of the estimated noise remains uncertain. Additionally, the noise was modeled as a normal distribution, whereas the experimental data exhibited slight skewness. If the actual noise is significantly smaller or larger than estimated, the optimization could produce designs that are either overly conservative or insufficiently robust.

8.7 Availability of information

Many of the identified limitations stem from the limited availability of detailed information from Biosphere, which is a consequence of the design still being in its early development stage and Biosphere being a start-up with limited budget. Beyond this project-specific context, a broader systemic challenge is the closed nature of many solar module supply chains. Manufacturers often treat technical specifications, material compositions, and production methods as proprietary information, resulting in limited publicly accessible data. This lack of transparency hinders independent evaluation and comparison of design choices, particularly with regard to circularity, reparability, and sustainability. Promoting more open data exchange in the solar industry would greatly benefit research, innovation, and responsible product development.

Given that incomplete information is a common characteristic of early-stage design processes, the outcomes of this optimization should not be interpreted as definitive solutions, but rather as a guiding framework for concept development. It is recommended that the optimization be revisited and refined in later design stages as more precise and comprehensive data becomes available.

9. Conclusion

This study presented a robust optimization methodology to enhance the mechanical strength of Biosphere's laminate-free photovoltaic (PV) module while maintaining a balance between repairability, weight, and costs. Recognizing that traditional laminated PV modules face significant challenges in terms of recyclability and repairability, Biosphere's alternative design eliminates the EVA encapsulation layer to facilitate easier disassembly and component reuse. However, this innovation comes at the expense of mechanical strength, necessitating a thorough optimization of critical design parameters.

A tailored Relative Repairability Assessment Method was developed for PV modules to quantify the impact of design changes on repairability, suitable for early-stage product development. It offers a complete and structured approach for identifying areas of improvement and making design tradeoffs that prioritize ease of repair. This method was integrated into a multi-objective optimization framework, alongside mass and cost metrics, to determine the most effective design modifications.

Another key element of this study was the implementation of the robust optimization algorithm Robustimizer to systematically account for uncertainties in the design process. Uncertainty estimates were derived from prototype verification tests in combination with Finite Element Analysis (FEA) in COMSOL, enabling to estimate the noise levels for critical parameters even in this early design phase. This approach reduced the dependence on overly conservative safety margins and limited the need for costly trial-and-error design iterations. The findings demonstrate that even limited physical testing can significantly enhance optimization precision compared to relying on generic safety factors.

The optimized design met the required mechanical strength, with an increase in repairability (+51%) and a decrease of the total costs (-9%). A main drawback is the increased mass of the module (+45%). Key improvements included thicker glass, a reduced quantity of adhesive dots, and moderately thinner frame, reflecting a careful trade-off between structural integrity and the circularity objectives of Biosphere.

The main takeaway from this study is that repairability, often overlooked in engineering optimization, can be meaningfully quantified and integrated into a multi-objective framework without compromising technical performance. Another main takeaway is that explicitly accounting for uncertainty enhances the robustness of the design and supports more informed decision-making, particularly when operating at the edge of technical feasibility. It shows that even in the context of early-stage product development where data is often incomplete and extensive testing is infeasible, a structured, simulation-based methodology and optimization can yield valuable design insights.

While the methodology proved effective, further refinement is necessary to enhance its accuracy and applicability. Several fundamental limitations were identified, including simplifications in the repairability model, assumptions in cost estimations, surrogate modeling approximations, limited data points during verification and the exclusion of dynamic and impact loading conditions. Most of these limitations are inherent to early-stage design optimizations, where data availability is limited. As such, the presented optimization should be considered a preliminary guideline to support informed, data-driven trade-offs rather than a definitive design solution.

Future work should focus on refining the repairability model with empirical data, expanding the scope to include dynamic and impact loads, and continuously updating cost models to reflect market developments. Furthermore, it is recommended to iteratively revisit the optimization as more precise data becomes available during subsequent design phases.

In conclusion, this research presents a practical method for optimizing early-stage PV module designs by balancing repairability with technical requirements. It offers a useful case study for startups and companies working on innovation in the renewable energy sector.

Acknowledgments I would like to thank my supervisor, Omid, for all our in-depth discussions, his supportive guidance and critical mindset. Additionally, I wish to thank Zola and all colleagues from Biosphere for their support and supervision throughout this project.

References

- [1] PVEDucation, "Module materials," 2024, URL: https://www.pveducation.org/pvcdrom/modules-and-arrays/module-materials.
- [2] IRENA International Renewable Energy Agency, "Record-breaking annual growth in renewable power capacity," 2025, URL: https://www.irena.org/News/pressreleases/2025/Mar/Record-Breaking-Annual-Growth-in-Renewable-Power-Capacity.
- [3] European Commission, "Here's new waste coming from the transition to renewables. how to reuse and recycle it?," 2025, URL: https://joint-research-centre.ec.europa.eu/jrc-news-and-updates/theres-new-waste-coming-transition-renewables-how-reuse-and-recycle-it-2025-03-11_en.
- [4] Clean Technica, "Nrel explodes solar panel waste myths," 2023, URL: https://cleantechnica.com/2023/10/13/nrel-explodes-solar-panel-waste-myths/.
- [5] S. Weckend, A. Wade, and G. Heath, "End-of-life management: Solar photovoltaic panels," *IEA-PVPS and IRENA*, 2016.

- [6] K. Wambach, "Photovoltaics recycling scoping workshop," 34th PV Specialists Conference, Philadelphia, 2009.
- [7] K. Sivagami *et al.*, "Solar panel recycling from circular economy viewpoint: A review," *Applied Solar Energy*, vol. 60, pp. 328–345, 2024.
- [8] J. Kirchherr and L. Piscicelli, "Towards an education for the circular economy (ece): Five teaching principles and a case study," *Resources Conservation and Recycling*, vol. 150, p. 104 406, 2019.
- [9] J. Dupuis, E. Saint-Sernin, O. Nichiporuk, P. Lefillastre, D. Bussery, and R. Einhaus, "Nice module technology from the concept to mass production: A 10 years review," *Conference Record of the IEEE Photovoltaic Specialists Conference*, pp. 003183–003186, 2012.
- [10] A. Majdi, M. Alqahtani, A. Almakytah, and M. Saleem, "Fundamental study related to the development of modular solar panel for improved durability and repairability," *IET Renewable Power Generation*, vol. 15, no. 7, pp. 1382–1396, 2021.
- [11] R. Einhaus et al., "Recycling and reuse potential of nice pv-modules," pp. 561–564, 2018.
- [12] International Electrotechnical Commission, "International standard iec 61215-1: Terrestrial photovoltaic (pv) modules design qualification and type approval," 2021.
- [13] E. Blanco-Espeleta, V. Pérez-Belis, and M. Bovea, "Repair index of energy-related products: Application to capsule coffee machines," *Sustainable Production and Consumption*, vol. 46, pp. 146–160, 2024.
- [14] M. Cordella, J. Sanfelix, and F. Alfieri, "Development of an approach for assessing the reparability and upgradability of energy-related products," *Procedia CIRP*, vol. 69, pp. 888–892, 2018.
- [15] E. Bracquené *et al.*, "Repairability criteria for energy related products study in the benelux context to evaluate the options to extend the product life time final report," 2018.
- [16] C. Spiliotopoulos *et al.*, "Product reparability scoring system: Specific application to smartphones and slate tablets," *Publications Office of the European Union*, 2022.
- [17] N. Rodríguez and C. Favi, "Eco-design guidelines takeaways from the analysis of product repairability and ease of disassembly: A case study for electric ovens," *Procedia CIRP*, vol. 105, pp. 595–600, 2022.
- [18] Austrian Standards, "Onr 192102: 2014 gütezeichen für langlebige, reparaturfreundlich konstruierte elektrische und elektronische geräte," 2024, URL: https://www.austrian-standards.at/de/shop/onr-192102-2014-10-01~p2091192.
- [19] The European Electrotechnical Committee for Standardization, "European standardization," 2024, URL: https://www.cencenelec.eu/.
- [20] Ministère de la transition ecologique, "Indice de réparabilité," 2024, URL: https://www.ecologie.gouv.fr/politiques-publiques/indice-reparabilite.
- [21] M. de la Transition écologique, "Instructions manual for the display and the calculation of the repairability index of electrical and electronic equipments," *Ministère de la Transition écologique*, 2022.
- [22] P. Vanegas *et al.*, "Ease of disassembly of products to support circular economy strategies," *Resources, Conservation and Recycling*, vol. 135, pp. 323–334, 2018.
- [23] F. D. Fazio, C. Bakker, B. Flipsen, and R. Balkenende, "The disassembly map: A new method to enhance design for product repairability," *Journal of Cleaner Production*, vol. 320, p. 128 552, 2021.

- [24] B. Flipsen, M. depypere, M. Huisken, and T. Opsomer, "Smartphone reparability scoring: Assessing the self-repair potential of mobile ict devices," *PLATE*, 2019.
- [25] S. Dangal, J. Faludi, and R. Balkenende, "Design aspects in repairability scoring systems: Comparing their objectivity and completeness," *Sustainability*, vol. 14, no. 14, 2022.
- [26] M. Cordella, F. Alfieri, and J. S. Forner, "Analysis and development of a scoring system for repair and upgrade of products," *EUR 29711 EN*, no. KJ-NA-29711-EN-N, 2019.
- [27] A. Chiralaksanakul and S. Mahadevan, "Reliability-based design optimization methods," *Journal of Mechanical Design*, pp. 851–857, 2004.
- [28] S. Choi, R. Canfield, and R. V. Grandhi, *Reliability-based Structural Design*. Springer London, 2007.
- [29] M. Valdebenito and G. Schueller, "A survey on approaches for reliability-based optimization," *Structural and Multidisciplinary Optimization*, vol. 42, no. 5, pp. 645–663, 2010.
- [30] O. Nejadseyfi, "Robustimizer: A graphical user interface application for efficient uncertainty quantification, robust optimization, and reliability-based optimization of processes and designs," *SoftwareX*, vol. 30, p. 102 077, 2025.
- [31] Apex, "Understanding tempered glass thickness: A comprehensive guide," URL: https://apextemperedglass.com/blog/tempered-glass-thickness/.
- [32] C. Barry, "Why glass sometimes breaks," IEEE, 2010.
- [33] COMSOL, "Performing a mesh refinement study," URL: https://www.comsol.com/support/knowledgebase/1261.
- [34] HZ Solar, "The fluctuating cost of solar pv modules: Understanding the price trends," 2024, URL: https://www.hzsolarsystem.com/a-the-fluctuating-cost-of-solar-pv-modules-understanding-the-price-trends.html.
- [35] D. Gearino, "Solar panel prices are rising again. here's why, and what may be next," 2025, URL: https://insideclimatenews.org/news/03042025/inside-clean-energy-solar-panel-prices-increase/.
- [36] M. Günaydın *et al.*, "Structural strength analysis of framed glass-glass photovoltaic module at different boundary conditions," 2020.
- [37] Y. Lee and A. Tay, "Stress analysis of silicon wafer-based photovoltaic modules under iec 61215 mechanical load test," *Energy Procedia*, vol. 33, pp. 265–271, 2013.

Appendix 1. Repairability assessment Biosphere PV Module Modifications
Appendix 1.1 Repairability of design parameter 1: Glass thickness

	Design parameter 1: glass thickness				
Parameter [Weight]	-1	0	1	Description	
Identification of the problem [2]	limits the ability to establish possi- ble causes of key failures by error	in the design parameter has no impact on the identification of the possible causes of key	design parame- ter ensures that more causes of key failures can by established	rather than sensors or systems influenced by physical dimensions. The process that is used for error detection is thus not influenced by glass thickness.	
maintenance	rameter reduces the availability of maintenance	no impact on the availability of maintenance	design param- eter increases the availability of maintenance and repair infor-	the repair process follows the same methods and steps, allowing the same maintenance and repair manuals to be used across different glass thicknesses. However, if	
Technical skills [1]	eter increases the reliance	in the design parameter has no impact on the technical skills needed for repair	the design pa- rameter reduces the need for	thicker variants, especially during replacement. On the	
spare parts [2]	causes the origi- nal and compat- ible parts to be more scarce	design parameter has no impact on the availability of spare parts	design parameter causes the original and compat-	Availability of specific sizes is not directly correlated with size itself. While smaller components can sometimes be harder to source, certain larger dimensions can also be	
Identification of parts [1]			An increase in the design parameter causes the parts to be more distinguishable from other parts		
•				Continued on next page	

	Design parameter 1: thicker glass (continued)					
Parameter [Weight]	-1	0	1	Description		
Disassembly and reassembly of parts [3]	eter increases the number of steps or time required for the disassembly and	in the design parameter has no impact on the time and amount of steps needed	eter decreases the number of steps or time required for the disassembly and	disassembly easier, as it requires less delicate handling. This likely results in a noticeable time saving, as the thin glass of Biosphere's current design requires extreme caution during (dis)assembly, especially when removing the frame. A thicker glass is expected to result in an easier frame removal, saving time. The increased weight		
parts [2]	rameter reduces the accessibility of parts for tools or machines	in the design parameter has no impact on the accessibility of parts with tools or machines	parts for tools or machines	age during disassembly, which generally improves the accessibility of other components without damage.		
Visibility of fas- teners [2]	reduces the visi- bility of fasteners	in the design	The design increases the visi- bility of fasteners used to assemble parts	The same fasteners can be used for different glass thicknesses.		
Removability of fasteners and disassembly reversibility [3]	reduces the re- versibility and/or	the design pa-	design parameter increases the re- versibility and/or reusability of the	The same fasteners can be used for different glass thicknesses.		
limitations [1]	limits on-site re- pairs of parts	design parameter has no impact on the possible re- pair locations	An increase in the design parameter facilitates on-site repairs of parts	which is very challenging to do on the spot with Biospheres original design and the used tools. This is particularly challenging for residential installations, such as rooftop systems. Thicker glass might make this even more challenging as it is heavier, but on the other hand the fact that thicker glass is less fragile might make it easier. Since the net effect of both factors is not (yet) tested, this criteria is given a score of 0.		
Degree of automation [2]	An increase in the design parameter reduces the au- tomatization pos- sibilities of the re- pairing process	in the design parameter has	An increase in the design parameter increases the au- tomatization pos- sibilities of the re- pairing process	tion, as the same methods and tools can be used for the repair.		
				Continued on next page		

	Design parameter 1: thicker glass (continued)					
Parameter [Weight]	-1	0	1	Description		
Types of ma-	design parame- ter increases the need for more	design parameter has no impact on the types of ma- chinery or tools	design param- eter decreases the need for	The same types of tools and machinery is needed for all glass thicknesses.		
State after re- pair/upgrade action [2]	in the design parameter has a negative impact on the quality (efficiency or	ter has no impact on the quality (efficiency or power output) and aesthetics of	in the design parameter has a positive impact on the quality (efficiency or	More research is needed regarding the degradation of the parts before during and after repair. For instance, repairs could potentially cause tiny, invisible cracks or defects in the glass. If this is the case, thicker glass might reduce this risk. However, since this has not yet been proven, this criterion is assigned a score of 0. Future research is needed in order to estimate this more accurately.		
Updatability [2]	An increase in the design parameter limits the possi- bility to replace parts for newer versions	has no impact on the possibility to replace parts for newer versions	An increase in the design parameter facili- tates upgrading parts for newer versions	Glass thickness does not affect upgradability, as long as the space between the glass sheets remains unchanged. However, if a thicker glass sheets would result in less space between the two sheets, it could limit the upgradability of the system, as larger versions of solar cells or electronics may not fit if there. The glass sheets themselves can easily be upgrated or replaced for other glass types or materials, regardless of thickness. arameter 1: glass thickness.		

Relative repairability score of glass thickness: 5/26. However, research is needed regarding the degradation of the parts due to repair.

Appendix 1.2 Repairability of design parameter 2: frame thickness

	Design parameter 2: frame thickness					
Parameter [Weight]	-1	0	1	Description		
Identification of	An increase in the	An increase	An increase in the	Frame thickness has no influence on the identification		
the problem [2]	design parameter	in the design	design parame-	of failures by error codes or manuals. For Biosphere's		
	limits the ability	parameter has	ter ensures that	design, the error detection is based on based software.		
	to establish possi-	no impact on the	more causes of	This is independent of frame thickness.		
			key failures can			
			by established			
	codes or descrip-	causes of key	by error codes or			
	tions in manuals	failures	descriptions in			
			manuals			
			ı	Continued on next page		

D			eter 2: frame thick	
Parameter [Weight]	-1	0	1	Description
Availability of maintenance	rameter reduces the availability of maintenance	in the design parameter has no impact on the availability of maintenance	design param- eter increases the availability of maintenance	ness, the repair process can likely follow the same meth- ods and steps, allowing the same maintenance and repair manuals to be used across different frame thicknesses. However, if the repair manuals include figures that depict
Technical skills [1]	eter increases the reliance	in the design parameter has no impact on the technical skills needed for repair	the design pa- rameter reduces the need for specialized skills	Frame thickness does not influence the skill level that is needed for repair.
Availability of spare parts [2]	causes the origi-	design parameter has no impact on the availability of	design parameter causes the origi- nal and compat-	Availability of specific frame sizes is not directly correlated with size itself. This is mainly due to the fact that only specific standardized sizes (30mm, 35mm and 40mm) are widely available on the market. Other dimensions are uncommon and need to be tailor made. However, this is regardless of their absolute size; both smaller and larger frames need tailor production.
Identification of parts [1]	design param- eter causes the	An increase in the design parameter has no impact on the identification of parts		All frame sizes are equally distinguishable from other components as other glass sheets.
•	design parameter increases the number of steps or time required for the disassembly and	An increase in the design parameter has no impact on the time and amount of steps needed for disassembly and reassembly of parts	design parameter decreases the number of steps or time required for the	such as a flathead screwdriver, inserted between the frame and the glass. A thicker and stiffer frame may make it more difficult to access this gap and remove the frame, while thinner frames may make it easier. However, it has
Accessibility of parts [2]	rameter reduces the accessibility	in the design	design parame- ter increases the accessibility of parts for tools or	
Visibility of fas- teners [2]	reduces the visi- bility of fasteners	An increase in the design parameter has no impact on the visibility of fasteners used to assemble parts	increases the visi- bility of fasteners used to assemble	Same fasteners can be used for all frame thicknesses. Continued on next page

Parameter	-1	0	eter 2: frame thick	Description
[Weight]	· ·	ľ	*	Description
Removability of	versibility and/or		increases the re- versibility and/or reusability of the	Same fasteners can be used for all frame thicknesses.
Repair location limitations [1]	design parameter		design parameter facilitates on-site	Frame thickness has no influence on the repair location possibilities as likely all frame thickness will use the same (dis)assembly methods and tools.
Degree of automation [2]	design parameter reduces the au-	in the design parameter has no impact on the	design parameter increases the au- tomatization pos- sibilities of the re-	In the original design, the frame must be removed manu ally because no machine currently exists that can do so without damaging the glass. This remains true regardless of frame thickness, meaning the frame does not influence the degree of automation.
Types of ma- chinery or tools needed [2]	design parame- ter increases the need for more	has no impact on the types of ma- chinery or tools	eter decreases the need for	It is expected that all frame thicknesses require the same disassembly methods and tools.
State after re- pair/upgrade action [2]	in the design parameter has a negative impact on the quality (efficiency or power output)	ter has no impact on the quality (efficiency or power output) and aesthetics of the product after	in the design parameter has a positive impact on the quality (efficiency or power output)	The frame thickness is expected to not influence the qual ity or aesthetics of the panel after repair. However, re search is needed to verify that thicker frames can be re moved from the glass without damaging the glass.
Updatability [2]	An increase in the design parameter limits the possi- bility to replace	An increase in the design parameter has no impact on the possibility to replace parts for newer versions	An increase in the design parameter facilitates upgrading	Frame thickness has no influence on updatability.

Table 9. Repairability assessment of design parameter 2: frame thickness.

Relative repairability score of frame thickness: 0/26. However, research is needed on the effects of frame thickness on the ease of (and state after) disassembly.

Parameter	Design parameter 3: amount of adhesive dots					
[Weight]	-1	0	1	Description		
Identification of the problem [2]	limits the ability to establish possi- ble causes of key failures by error	in the design parameter has no impact on the identification of the possible causes of key	design parame- ter ensures that more causes of key failures can by established	The amount of adhesive dots has no influence on the identification of failures. Error detection for the Biosphere PV module design is based on software. Whether a panel has a lot of adhesive dots or none at all, the software remains the same.		
maintenance	rameter reduces the availability of maintenance	in the design parameter has no impact on the availability of maintenance and repair information	design parameter increases the availability of maintenance and repair information (printed or online)	The amount of adhesive dots has no influence on the availability of maintenance and repair information. Assuming the overall design stays the same with different amounts of adhesive dots, the repair process follows the same methods and steps, allowing the same maintenance and repair manuals to be used across different adhesive dot quantities. However, if the repair manuals include figures that depict a different adhesive dot amounts than in the panel being repaired, this could cause confusion. To avoid misunderstandings, it is recommended to create a new manual for each dot configuration, or to make a new manual that includes all common dot configurations.		
Technical skills [1]	eter increases the reliance	in the design parameter has no impact on the technical skills needed for repair	the design pa- rameter reduces the need for specialized skills	The amount of adhesive dots does not influence the skill level that is needed for repair, as the same methods and tools can be used for all adhesive dot quantities.		
Availability of spare parts [2]	design parameter causes the origi-	design parameter has no impact on the availability of	design parameter causes the origi- nal and compat-	An increase in adhesive dots requires more PIB, but since the types of parts and materials remain the same, this does not impact the scarcity of the used components. A larger quantity of PIB is expected to be approximately as available as a smaller quantity.		
parts [1]	design parameter causes the parts to be less distinguishable from other parts	design parameter has no impact on the identification of parts	design parameter causes the parts to be more distinguishable from other parts			
	eter increases the number of steps or time required for the disassembly and	in the design parameter has	design parameter decreases the number of steps or time required for the disassembly and	A bigger quantity of dots will require more time to disassemble and reassemble the panel, as each extra dot must be manually removed and extruded, which is one of the most time-consuming steps. Continued on next page		

	Design parameter 3: amount of adhesive dots (continued)					
Parameter [Weight]	-1	0	1	Description		
Accessibility of parts [2]	rameter reduces the accessibility	in the design	design parame- ter increases the accessibility of parts for tools or machines			
Visibility of fas- teners [2]	design parameter reduces the visibility of fasteners	in the design parameter has no impact on	increases the visi- bility of fasteners	The dots are already easily distinguishable from the surrounding components, as the black-colored adhesive dots hold copper-colored wires and transparent glass. The quantity of the dots is unlikely to affect the visibility. Additionally, since the dots do not determine the type of other fasteners used, they have no impact on the visibility of the other fasteners.		
fasteners and disassembly reversibility [3]	design parameter reduces the re- versibility and/or reusability of the connections	the design pa- rameter has no impact on the re- versibility and/or reusability of the connections	design parameter increases the re- versibility and/or reusability of the connections			
Repair location limitations [1]		An increase in the design parameter has no impact on the possible re- pair locations	design parameter facilitates on-site	For larger amounts of dots, it will take more effort and time to manually remove and replace them, which is not desirable especially in uncomfortable positions on rooftop systems. However, it does not influence whether or not the repair is theoretically possible in those locations.		
Degree of automation [2]	reduces the au-	in the design parameter has no impact on the	design parameter increases the au- tomatization pos- sibilities of the re-	Even though some steps might be more difficult or take more time, see <i>Disassembly and reassembly of parts</i> , the same steps and methods can be used for all adhesive dot quantities. Therefore the amount of adhesive dots has no influence on the degree of automation.		
	design parame- ter increases the need for more advanced or	An increase in the design parameter has no impact on the types of ma- chinery or tools needed	design param- eter decreases the need for advanced or			
				Continued on next page		

	Design parameter 3: amount of adhesive dots (continued)					
Parameter	-1	0	1	Description		
[Weight]						
State after re-	An increase	An increase in the	An increase	For now the product appears to be fully restorable to		
pair/upgrade	in the design	design parame-	in the design	its original functionality when repaired efficiently and		
action [2]				with care and there is no prove the amount of adhesive		
	negative impact	on the quality	positive impact	dots will influence this. However, the adhesive dots can		
	on the quality	(efficiency or	on the quality	leave small residues after removal. It must be investigated		
	(efficiency or	power output)	(efficiency or	whether remains of the adhesive dots impact efficiency;		
	power output)	and aesthetics of	power output)	or wether the remains impact the adhesive strength of		
	and aesthetics of			new dot layers. Also, possible remains may influence the		
	the product after	repair	the product after	aesthetics of the panel after repair.		
	repair		repair			
Updatability [2]	An increase in the	An increase in the	An increase	An increased number of adhesive dots between the glass		
	design parameter	design parameter	in the design	sheets and solar cells reduces the available space. This		
				could potentially limit the upgradability of the system, as		
	bility to replace	the possibility to	tates upgrading larger versions of solar cells or electronics may			
	parts for newer	replace parts for	parts for newer	there is insufficient space between the dots.		
	versions		versions			

 Table 10. Repairability assessment of design parameter 3: amount of adhesive dots.

Relative repairability score of amount of adhesive dots: -8/26. Research needed into the state after repair.

Appendix 1.4 Repairability of design parameter 4: Distance between mounting clamps

Parameter [Weight] Identification of the problem [2] An increase in the design parameter limits the ability to establish possible causes of key failures by error codes or descriptions in manuals Availability of maintenance and repair information [1] Availability of maintenance and repair information [1] Availability of maintenance and repair information (printed or online) Availability of maintenance and repair information (printed or online) An increase in the design parameter educes the design parameter has no impact on the design parameter has no impact on the availability of maintenance and repair information (printed or online) An increase in the design parameter enduces in the design parameter has no impact on the availability of maintenance and repair information (printed or online) An increase in the design parameter enduces in the design parameter has no impact on the availability of maintenance and repair information (printed or online) An increase in the design parameter enduces in the design parameter has no impact on the design parameter has no impact on the availability of maintenance and repair information. An increase in the design parameter enduces in the design parameter has no impact on the design parameter has no impact on the design parameter has no impact on the availability of maintenance and repair information. Regardless of the location of the mounting clamps is independent on the availability of maintenance and repair information. Regardless of the location of the mounting clamps is independent on the availability of maintenance and repair information. Regardless of the location of the mounting clamps is independent on the availability of maintenance and repair information. Regardless of the location of the mounting clamps is independent on the availability of maintenance and repair information. Regardless of the location of the mounting clamps independent on the availability of maintenance and repair information. Regardless of the location of the mounting clamps indep		Design parameter 4: distance betwen mounting clamps					
the problem [2] design parameter limits the ability to establish possible causes of key failures by error codes or descriptions in manuals and repair information [1] Availability of maintenance and repair information [1] An increase in the design parameter has no impact on the interest of maintenance and repair information (printed mation (printed) An increase in the design parameter has no impact on the design parameter has in the design parameter has and repair information (printed) An increase in the design parameter has in the design parameter reduces the availability of maintenance and repair information. Regardless of the location of the mounting clamps, the repair manuals to be used. However, if the repair manuals include figures that depict a different clamp-		-1	0	1	Description		
maintenance and repair information. the design parameter reduces information [1] the availability of maintenance and repair information. Regardless of the location of the mounting clamps, the availability of maintenance and repair information. Regardless of the location of the mounting clamps, the repair process follows the same methods and steps for all clamping locations, allowing the same maintenance and repair information. Regardless of the location of the mounting clamps, the repair process follows the same methods and steps for all clamping locations, allowing the same maintenance and repair manuals to be used. However, if the repair manuals include figures that depict a different clamp-		design parameter limits the ability to establish possi- ble causes of key failures by error codes or descrip-	in the design parameter has no impact on the identification of the possible causes of key	design parame- ter ensures that more causes of key failures can by established by error codes or descriptions in	identification of failures.		
could cause confusion. To avoid misunderstandings, it is recommended to include different possible clamping configurations in the manual.	maintenance and repair	the design pa- rameter reduces the availability of maintenance and repair infor-	in the design parameter has no impact on the availability of maintenance	design param- eter increases the availability of maintenance and repair infor-	the availability of maintenance and repair information. Regardless of the location of the mounting clamps, the repair process follows the same methods and steps for all clamping locations, allowing the same maintenance and repair manuals to be used. However, if the repair manuals include figures that depict a different clamping configurations than in the panel being repaired, this could cause confusion. To avoid misunderstandings, it is recommended to include different possible clamping		

Dawawastaw		i parameter 4: uist		unting clamps (continued)
Parameter [Weight]	-1	U	1	Description
Technical skills [1]	eter increases the reliance	in the design parameter has no impact on the technical skills needed for repair	the design pa- rameter reduces the need for	The location of the clamps does not influence the skill level that is needed for repair, as the same methods and tools can be used for all locations.
Availability of spare parts [2]	design parameter causes the origi-	design parameter has no impact on the availability of		The location of the clamps does not influence the type and amount of materials or parts needed.
Identification of parts [1]	design param- eter causes the parts to be less	An increase in the design parameter has no impact on the identification of parts	design param- eter causes the	The location of the clamps does not affect the identification of parts.
,	eter increases the number of steps or time required for the disassembly and		design parameter decreases the number of steps or time required for the disassembly and	The location of the clamps does not affect the time or steps required for disassembling and reassembling the panel.
Accessibility of parts [2]	rameter reduces the accessibility	in the design parameter has no impact on the	design parame- ter increases the accessibility of parts for tools or	The location of the clamps does not affect the accessibility. Except for the junction box which can directly be access without removing the clamps, all other components require the clamps to be removed for repair, regardless of their placement.
teners [2]	reduces the visi- bility of fasteners used to assemble parts	in the design parameter has no impact on the visibility of fasteners used to assemble parts	increases the visi- bility of fasteners used to assemble parts	
fasteners and disassembly reversibility [3]	design parameter reduces the re- versibility and/or reusability of the connections	the design pa- rameter has no impact on the re- versibility and/or reusability of the connections	design parameter increases the re- versibility and/or reusability of the connections	The location of the clamps does not impact the removability or reusability of the fasteners.
Repair location limitations [1]		design parameter	design parameter	The location of the mounting clamps does not influence the repair location possibilities, as the same methods and tools can be used for all locations.
				Continued on next page

	Design parameter 4: distance between mounting clamps (continued)					
Parameter	-1	0	1	Description		
[Weight]						
	An increase in the	An increase	An increase in the	The location of the mounting clamps does not influence		
tomation [2]				the degree of automation, as the same methods and tools		
				can be used for all clamping locations.		
		no impact on the				
	sibilities of the re-	automatization	sibilities of the re-			
	pairing process	possibilities of	pairing process			
		the repairing				
		process				
Types of ma-	An increase in the	An increase in the	An increase in the	The same methods and tools can be used for all mounting		
chinery or tools	design parame-	design parameter	design param-	clamp locations.		
needed [2]		has no impact on	eter decreases			
	need for more	the types of ma-	the need for			
	advanced or	chinery or tools	advanced or			
	specialized tools	needed	specialized tools			
	or machines		or machines,			
	(like tailored		meaning more			
	machines or		basic tools (like			
	product-specific		flathead and hex			
	tools) to repair		drivers) can be			
	parts		used to repair			
			parts			
State after re-		An increase in the		The mounting clamps are expected to not impact the the		
pair/upgrade			in the design			
action [2]			parameter has a	product after repair.		
		on the quality				
	on the quality		on the quality			
	'	power output)	•			
		and aesthetics of				
		the product after				
	the product after	repair	the product after			
	repair		repair			
Updatability [2]		An increase in the		The mounting clamps are expected to not impact the the		
	0 .	0 .	0	updatability of the panel.		
		•				
		the possibility to	tates upgrading			
	•	replace parts for				
	versions	newer versions	versions			

Relative repairability score of the distance between mounting clamps: 0/26.

Appendix 1.5 Repairability of design parameter 5: width of mounting clamps

		Design param	eter 5: width of m	ounting clamps
Parameter [Weight]	-1	0	1	Description
the problem [2]	limits the ability to establish possi- ble causes of key failures by error	in the design parameter has no impact on the identification of the possible causes of key	design parame- ter ensures that more causes of key failures can by established	The design and dimensions of the mounting clamps do not influence the identification of failures.
Availability of maintenance and repair information [1]	rameter reduces the availability of maintenance	in the design parameter has no impact on the availability of maintenance	design param- eter increases the availability of maintenance and repair infor-	The design or dimensions of the mounting clamps is independent on the availability of maintenance and repair information. It might be that figures in the available repair information show different mounting clamps, but the repair process follows the same methods and steps for all clamp types, allowing the same maintenance and repair manuals to be used. However, if the repair manuals include figures that depict a different mounting clamps than in the panel being repaired, this could cause confusion. To avoid misunderstandings, it is recommended to make a new manual that includes all the different possible clamping configurations.
Technical skills [1]	eter increases the reliance	in the design parameter has no impact on the technical skills needed for repair	the design pa- rameter reduces the need for	The design and dimensions of the clamps do not influence the skill level that is needed for repair, as the same methods and tools can be used for all locations.
Availability of spare parts [2]	design parameter causes the origi-	design parameter has no impact on the availability of	design parameter causes the origi- nal and compat-	The design and dimensions of the clamps does not influence the availability. This is mainly due to the fact that only the standardized size of 50mm is widely available on the market while all other dimensions, whether smaller or larger, would be tailor-made. Hence, there is no correlation between mounting clamp size and availability.
Identification of parts [1]	design param- eter causes the	design parameter has no impact on the identification of parts	design parameter causes the parts to be more distinguishable from other parts	The design and dimensions of the clamps does not affect the identification of parts. Bigger mounting clamps are equally distinguishable from other components as smaller mounting clamps.
	eter increases the number of steps or time required for the disassembly and	in the design parameter has	design parameter decreases the number of steps or time required for the disassembly and	
				Continued on next page

g clamps (continued) Description	1	0	-1	Parameter
Description	1	U	-1	[Weight]
The design and dimensions of the clamps does not affect the accessibility. Except for the junction box which can directly be access without removing the clamps, all other components require the clamps to be removed for repair regardless of the mounting clamp dimensions.	design parame- ter increases the accessibility of parts for tools or	in the design parameter has no impact on the	rameter reduces the accessibility	
The design and dimensions of the clamps does not affect the visibility of the fasteners.	increases the visi- bility of fasteners used to assemble		reduces the visi- bility of fasteners	Visibility of fas- teners [2]
The design and dimensions of the clamps does not impact the removability or reusability of the fasteners.	design parameter increases the re- versibility and/or reusability of the		design parameter reduces the re- versibility and/or	,
The design and dimensions of the clamps do not influence the repair location possibilities, as the same methods and tools can be used for all clamp sizes.	An increase in the design parameter facilitates on-site repairs of parts	An increase in the design parameter has no impact on the possible re- pair locations		Repair location limitations [1]
The design and dimensions of the mounting clamps do not influence the degree of automation, as the same methods and tools can be used for all dimensions.	increases the au-	in the design	reduces the au-	Degree of automation [2]
The same methods and tools can be used for all mounting clamp sizes.	design param- eter decreases the need for	design parameter has no impact on the types of ma- chinery or tools	design parame- ter increases the need for more	Types of ma- chinery or tools needed [2]
	drivers) can be used to repair		tools) to repair	

	Design parameter 5: width of mounting clamps (continued)						
Parameter	-1	0	1	Description			
[Weight]							
State after re-		An increase in the		The mounting clamps are expected to not impact the the			
pair/upgrade	in the design	design parame-	in the design	quality (efficiency or power output) and aesthetics of the			
action [2]	parameter has a	ter has no impact	parameter has a	product after repair.			
			positive impact				
	on the quality	(efficiency or	on the quality				
	(efficiency or	power output)	(efficiency or				
			power output)				
	and aesthetics of	the product after	and aesthetics of				
	the product after	repair	the product after				
	repair		repair				
Updatability [2]	An increase in the	An increase in the	An increase	The mounting clamps are expected to not impact the the			
	design parameter	design parameter	in the design	updatability of the panel.			
	limits the possi-	has no impact on	parameter facili-				
	bility to replace	the possibility to	tates upgrading				
	parts for newer	replace parts for	parts for newer				
	versions		versions	otor Et width of mounting clamps			

 Table 12. Repairability assessment of design parameter 5: width of mounting clamps.

Relative repairability score of mounting clamp width: 0/26.

Appendix 2. Material properties

Table 13. Material properties used in the model and their sources.

Material	Material property	Used value	From
Aluminium 6083-T6	Density	2700 kg/m ³	COMSOL
	Young's modulus	69 GPa	COMSOL
	Poisson ratio	0.33	COMSOL
	Yield strength	215 MPa	COMSOL
	Tensile strength	240 MPa	COMSOL
Schott solar glass	Density	2500kg/m³	COMSOL
	Young's modulus	74.8 GPa	CES Edupack
	Poisson ratio	0.216	COMSOL
	Design yield strength	42 MPa	[36]
	Tensile strength	90–170 MPa	Strength depends on used glass type [36]
Polyisobutylene (PIB)	Density	1000 kg/m ³	COMSOL
	Young's modulus	10 MPa	CES Edupack
	Poisson ratio	0.48	CES Edupack
	Yield strength	2.4 MPa	CES Edupack
	Tensile strength	9 MPa	CES Edupack
Silicon (monocrystalline)	Density	2329 kg/m³	COMSOL
	Young's modulus	185 GPa	CES Edupack
	Poisson ratio	0.22	CES Edupack
	Yield strength	200 MPa	CES Edupack
	Tensile (bending) strength	200 MPa	[37]

Appendix 3. Mesh convergence

Table 14. Mesh convergence study showing deflection and stress values at three probe points for various mesh sizes. Probe 2 and Probe 3 are place near the mounting clamp, while probe 1 is placed in the middle of the module. The "finer" mesh setting was selected to achieve a balance between computational efficiency and sufficient simulation accuracy.

Mesh size	Deflection [mm]	Stress Probe 1 [MPa]	Stress Probe 2 [MPa]	Stress Probe 3 [MPa]
Coarser	153	25.7	225.1	215.3
Coarse	171	28.3	223.6	216.5
Normal	174	30.3	273.4	209.1
Fine	177	29.9	270.1	251.6
Finer	178	28.2	272.5	250.4
Finest	178	28.9	272.1	252.1

Appendix 4. Optimum improvement

Table 15. Normalized parameter values for the optimum design after each iteration. An additional DOE was added near the predicted optimum in each step to refine the surrogate model and improve accuracy.

	Hframe	Wclamp	Dmounting	Hglass1	Hglass2	DdotsX	DdotsY
Optimum 1st iteration	0.1915	0.4452	0.0000	0.5208	1.0000	0.9385	0.0000
Optimum 2nd iteration	0.1841	0.4043	0.0000	0.5695	1.0000	1.0000	0.0000
Optimum 3rd iteration	0.1900	0.4042	0.0000	0.5083	1.0000	1.0000	0.0000